# Response to Comments of Reviewer #1

**Manuscript number:** acp-2019-935
**Authors:** Cheng Gong, Yadong Lei, Yimian Ma, Xu Yue and Hong Liao
**Title:** Ozone-vegetation feedback through dry deposition and isoprene emissions in a global chemistry-carbon-climate model

*Gong et al. present research using the NASA ModelE2-YIBs model to estimate the impact of ozone damage to vegetation on atmospheric composition. They implement a more detailed representation of ozone damage in a coupled land-atmosphere model and find that, in general, inhibition to stomatal conductance leads to ozone increases. Quantifying biosphere-atmosphere exchange processes such as ozone damage in coupled models is an important line of research, and this work will likely be fit for publication in ACP once the following comments are addressed.*

**Response:**

Thank you for the helpful comments and suggestions. We have revised the manuscript carefully and the point-to-point responses are listed below.

**General comments:**

*My major concern is with seemingly inconsistent results in various heavily vegetated areas, specifically Africa. In Figure 2, ozone concentrations in central Africa look to be ~48 ppbv in a region with a lot of vegetation. This is higher than ozone in other regions (e.g. North America) that do show ozone damage impacts. However, in Figures 3, 5, 7, and 8, there are no discernable ozone damage impacts shown in this area. Why is that the case? This is surprising and should be explained further in the manuscript.*

**Response:**

Sorry for the confusion due to the low resolution of figures. If we zoom in Figure 2 on Africa (Figure R1), the 'heavily vegetated areas' (enclosed by the green rectangle), which is mainly covered by evergreen broadleaf forest (Figure R2), show low $O_3$ concentrations. Meanwhile, the region with high $O_3$ concentrations (enclosed by the blue rectangle) show quite low GPP and IPE. As a result, the weak $O_3$-vegetation interactions are reasonable in Africa.

In Sitch et al. (2007) schemes, different vegetation types show different performance to the $O_3$ exposure. Compared with evergreen or deciduous broadleaf forest, C3/C4 grassland and cropland have higher threshold $F_{O3,crit}$ (Supplementary Table S1). As a result, C3/C4 grassland and cropland in African would suffer lower level of $O_3$ damage than the deciduous broadleaf forest in North America even under the similar level of $O_3$ exposure, leading to trivial ozone damage impacts in African in Figure 3, 5, 7, and 8.

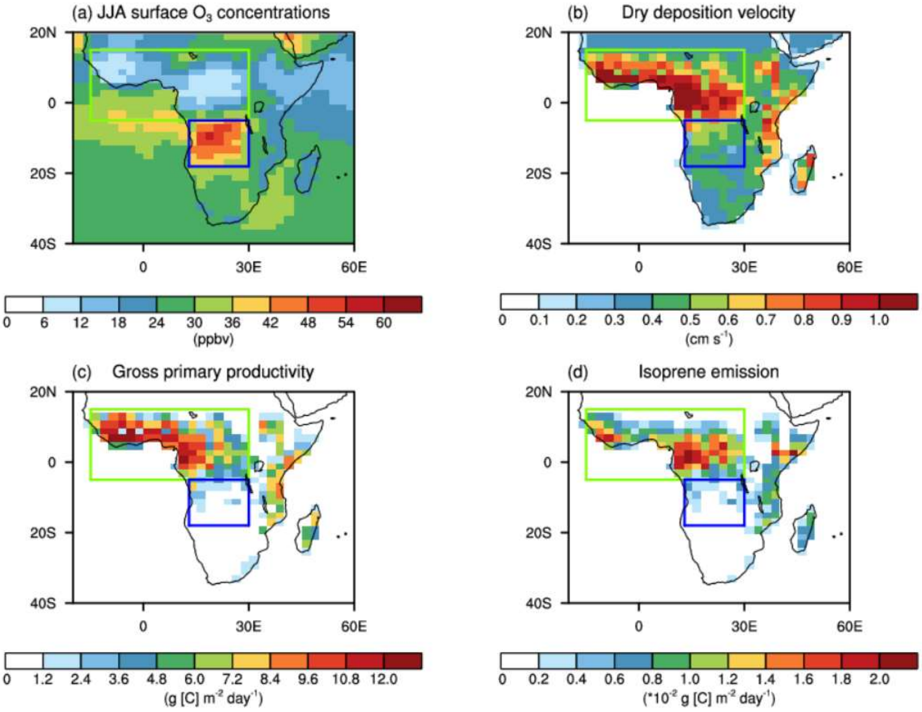

Figure R1. The same as Figure 2 but zoomed in on Africa. The green box encloses the ‘heavy vegetated areas’ with high GPP and IPE. The blue box encloses areas where surface $O_3$ concentrations are high.

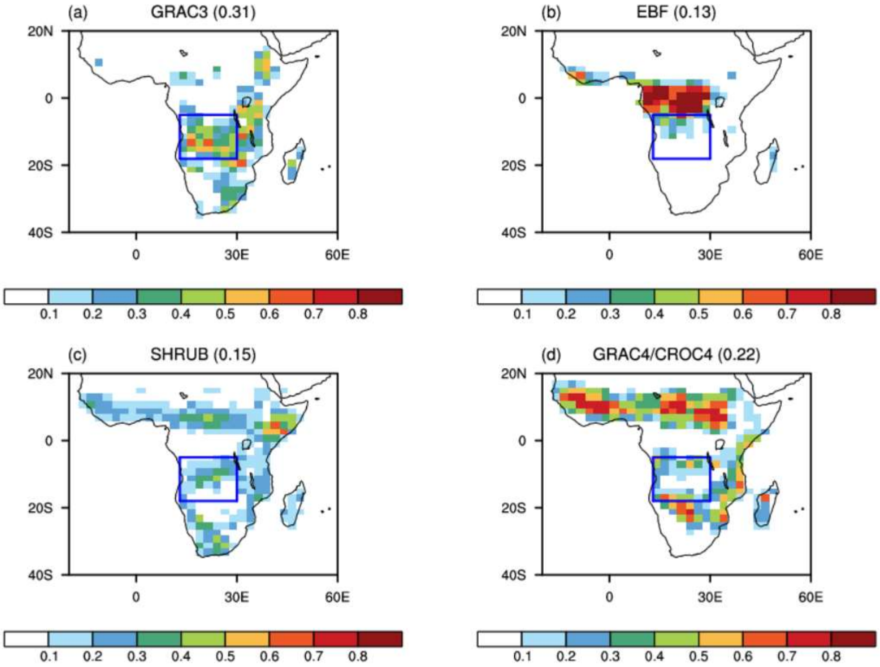

Figure R2. Land cover fraction of (a) C3 grassland , (b) evergreen broadleaf forest, (c) shrubland and (d) C4 grassland and cropland. The average cover of each PFT over the areas with high surface $O_3$ concentrations (blue box) is given in the subtitles.

**Specific Comments:**

*P2 L31: Citation needed for the statement that the majority of ozone deposition is through stomatal pathways.*

**Response:**

The sentence has been revised as:

'$O_3$ dry deposition is one of the important sink of tropospheric $O_3$ and mainly occurs over vegetation (Wesely, 1989). The stomatal uptake of vegetation plays an important role in this removal process. (Wesely and Hicks, 2000)' (Page 3, Lines 1-2)

*P3: Despite the text critical of previous work, the authors here find a very similar ultimate impact of ozone damage on vegetation. This should be acknowledged here or elsewhere in the manuscript.*

**Response:**

We have added the correspondingly statement in the second paragraph of Sect.4 Conclusion and discussion:

'Sadiq et al. (2017) also showed positive $O_3$-vegetation feedback on the surface $O_3$ in a global model. Compared to their results, we find an ultimate positive feedback with similar magnitude of surface $O_3$ concentrations but different spatial pattern. The strongest feedback in eastern China….' (Page 12, Lines 25-27)

*P4: A description of biogenic emissions is necessary in this section.*

**Response:**

The description of biogenic emissions has been added in the second paragraph in Sect. 2.1:

'…The LAI and tree growth are dynamically simulated with the allocation of carbon assimilation. The emissions of isoprene are calculated online as a function of Je photosynthesis (Eq. (1)), canopy temperature, intercellular $CO_2$, and $CO_2$ compensation point (Arneth et al., 2007; Unger, 2013), and have been fully validated by Unger et al. (2013). Carbon fluxes, phenology, LAI, GPP, and net ecosystem exchange (NEE), ….' (Page 5, Lines 1-5)

*P6 Eq 10: What are the variables "n" and "i"?*

**Response:**

The Eq. (10) in origin manuscript and the correspondingly explanation has been revised as:

$$\mathrm{POD}_1 = \int_1^n (\mathrm{F}_{\mathrm{O}_3} - 1)\mathrm{dt}$$

(14)

'where $F_{O3}$ is the $O_3$ uptake rate by stomata (nmol $O_3$ $m^{-2}$ $s^{-1}$), which is the same as that in Eq. (11). *dt* indicates the time integration step and *n* indicates the total number of time steps during the growing season.' (Page 7, Lines 10-13)

*P6 L28: What does "because of the data limit" mean?*

**Response:**

As we described above, 'To date, only one study (Yuan et al., 2017) has explored the responses of IPE to different levels of $O_3$ damage for two poplar clones', so here we have to apply the PDI function for all vegetation types even though it is based on poplar observations. We have revised this sentence to clarify:

'Limited by the data availability, we apply the PDI function (Eq. (13)) for poplar to all vegetation types as follow:' (Page 7, Lines 16-17)

*P7: The CTRL statement as described here is confusing. The text states that damage is calculated offline using the Sitch et al. (2007) scheme, but Table 1. states "None". Which is it?*

**Response:**

Sorry for the confusion.

The CTRL run calculates offline ozone damaging, which does not feed back to affect vegetation growth and the stomatal uptake of ozone. As a result, we denote "None" for this run in original Table 1. To clarify, we change "None" in Table 1 to "Offline". In text, we revised as follows:

'In the CTRL run, the effects of $O_3$ damage to photosynthesis, stomatal conductance, and IPE are calculated offline; such damages are not fed back to affect vegetation growth and dry deposition of $O_3$.' (Page 7, Lines 27-29)

*P7 L30: The linear fit in Figure 7d indicates and absolute bias of 32 ppbv. This should be acknowledged in the text as a limitation of this modeling approach.*

**Response:**

The sentences have been revised as follow:

'Figure 1 shows a comparison of the simulated summer $O_3$ concentrations to the observations. The model in general captures reasonable spatial patterns with a correlation coefficient of 0.41. The NMBs between simulations and observations in U.S and Europe are 11.7% and 13.2%, respectively, which are comparable with the simulation performed by CESM (Lamarque et al., 2012; Sadiq et al., 2017). However, the model overestimates $O_3$ concentrations by 29.3% with a regression intercept of 32 ppbv, suggesting that simulated $O_3$ vegetation damage might be overestimated especially over some regions with low ambient $O_3$ level. The large overestimate is mainly a result of overestimation in China…' (Page 8, Lines 17-22)

*P9 L10: If the justification for focusing on northern hemispheric summer is that absolute changes to IPE are most significant during this time, why not show this in a figure instead of merely suggesting it?*

**Response:**

A new supplementary Figure S4 is added to show the absolute changes in IPE:

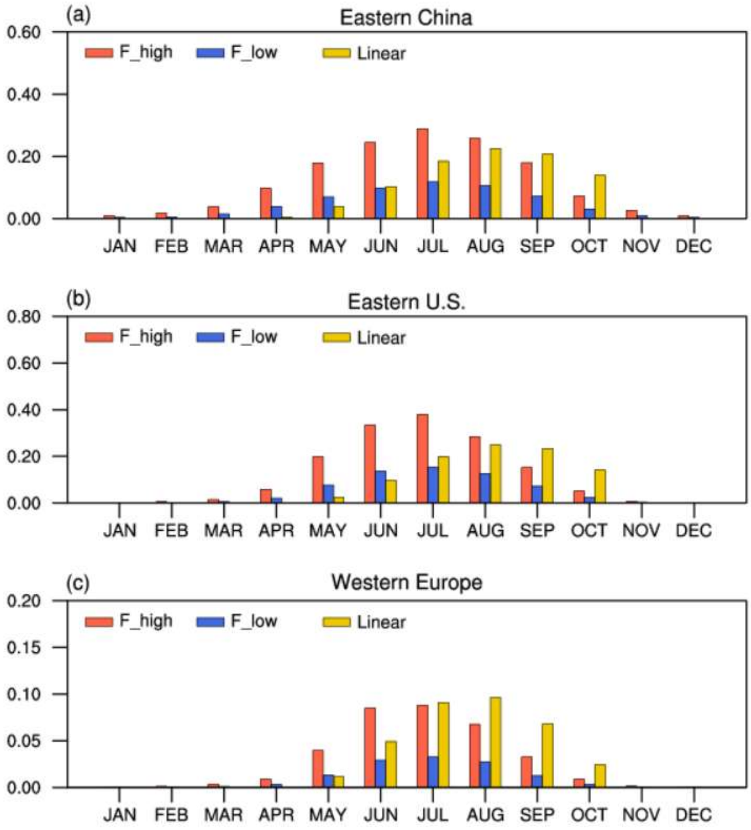

Supplementary Figure S4. Monthly mean absolute $O_3$ damage to IPE ($10^{-2}$ g[C] $m^{-2}$ $day^{-1}$) averaged over (a) eastern China, (b) the eastern U.S. and (c) western Europe by using the F scheme with high/low sensitivities and the linear scheme, respectively.

The main reason for focusing on boreal summer is that surface $O_3$ concentrations are high and vegetation grows vigorously in the northern hemisphere. Consequently, the $O_3$-vegetation-IPE interactions are supposed to be the strongest. In the text, we clarify as follows:

'…However, the IPE peaks during summer (Fig. S3), suggesting that absolute changes in IPE are most significant during this season (Fig. S4). Meanwhile, since the surface $O_3$ concentrations and the vegetation growth both peak during boreal summer in northern hemisphere, the $O_3$-vegetation interactions are supposed to be the strongest in this season. As a result, we focus our analyses on the summer to explore the $O_3$-vegetation interactions and feedback.' (Page 10, Lines 1-5)

*P10 L10: The authors speculate that the changes are no due to IPE changes, but instead meteorology. This should be explained further in more detail or stated more clearly as speculation.*

**Response:**

The sentence has been revised as follow:

‘Nevertheless, inclusion of IPE reductions helps increase surface $O_3$ over the eastern U.S. (Figs. 5d/5f vs. Fig. 5b), which is unexpected since the reduction in IPE is supposed to decrease $O_3$ concentrations. These changes are speculated to be indirectly related to $O_3$-vegetation feedback to meteorology and would be further examined in the next section.’ (Page 11, Lines 4-6)

*P11 L22: “likely related to the increased temperature…” further speculation. The sensitivity of the simulated ozone to temperature is not disentangled from other confounding factors. This should either be explicitly done, or the statement softened*

**Response:**

The sentence has been revised as follow:

‘The increased temperature following reduced SOA concentrations are speculated as a possible cause for this result.’ (Page 12, Lines 19-20)

## References

Arneth, A., Niinemets, U., Pressley, S., Back, J., Hari, P., Karl, T., Noe, S., Prentice, I. C., Serca, D., Hickler, T., Wolf, A., and Smith, B.: Process-based estimates of terrestrial ecosystem isoprene emissions: incorporating the effects of a direct CO2-isoprene interaction, Atmospheric Chemistry and Physics, 7, 31-53, 10.5194/acp-7-31-2007, 2007.

Lombardozzi, D., Levis, S., Bonan, G., and Sparks, J. P.: Predicting photosynthesis and transpiration responses to ozone: decoupling modeled photosynthesis and stomatal conductance, Biogeosciences, 9, 3113-3130, 10.5194/bg-9-3113-2012, 2012

Sadiq, M., Tai, A. P. K., Lombardozzi, D., and Martin, M. V.: Effects of ozone-vegetation coupling on surface ozone air quality via biogeochemical and meteorological feedbacks, Atmospheric Chemistry and Physics, 17, 3055-3066, 10.5194/acp-17-3055-2017, 2017.

Sitch, S., Cox, P. M., Collins, W. J., and Huntingford, C.: Indirect radiative forcing of climate change through ozone effects on the land-carbon sink, Nature, 448, 791-U794, 10.1038/nature06059, 2007.

Unger, N.: Isoprene emission variability through the twentieth century, Journal of Geophysical Research-Atmospheres, 118, 13606-13613, 10.1002/2013jd020978, 2013.

Unger, N., Harper, K., Zheng, Y., Kiang, N. Y., Aleinov, I., Arneth, A., Schurgers, G., Amelynck, C., Goldstein, A., Guenther, A., Heinesch, B., Hewitt, C. N., Karl, T., Laffineur, Q., Langford, B., McKinney, K. A., Misztal, P., Potosnak, M., Rinne, J., Pressley, S., Schoon, N., and Seraca, D.: Photosynthesis-dependent isoprene emission from leaf to planet in a global carbon-chemistry-climate model, Atmospheric Chemistry and Physics, 13, 10243-10269, 10.5194/acp-13-10243-2013, 2013

Wesely, M. L.: PARAMETERIZATION OF SURFACE RESISTANCES TO GASEOUS DRY DEPOSITION IN REGIONAL-SCALE NUMERICAL-MODELS, Atmospheric Environment, 23, 1293-1304, 10.1016/0004-6981(89)90153-4, 1989.

Wesely, M. L., and Hicks, B. B.: A review of the current status of knowledge on dry deposition, Atmospheric Environment, 34, 2261-2282, 10.1016/s1352-2310(99)00467-7, 2000.

Yuan, X., Feng, Z., Liu, S., Shang, B., Li, P., Xu, Y., and Paoletti, E.: Concentration- and flux-based dose-responses of isoprene emission from poplar leaves and plants exposed to an ozone concentration gradient, Plant Cell and Environment, 40, 1960-1971, 10.1111/pce.13007, 2017

# Response to Comments of Reviewer #2

**Manuscript number:** acp-2019-935
**Authors:** Cheng Gong, Yadong Lei, Yimian Ma, Xu Yue and Hong Liao
**Title:** Ozone-vegetation feedback through dry deposition and isoprene emissions in a global chemistry-carbon-climate model

*This study considers the impacts on surface ozone concentrations due to two ozone vegetation feedback mechanisms, the dry deposition inhibition by ozone and the isoprene emission inhibition by ozone. This is an important scientific question that have been tackled by several previous studies. The unique aspect of this work is that the two feedback mechanisms are explicitly included in the ModelE2-YIBs model, and two levels of parameterized sensitivity were assessed for each of the two feedback mechanisms. The results show that the ozone-inhibition of dry deposition generally wins over the effects of ozone-inhibition of isoprene emissions, such that surface ozone increase over Eastern US, Europe, and Eastern China when the ozone effects are considered, relative to the control simulation (where no ozone effects are considered). In addition, indirect impacts on meteorology via weakened transpiration and enhanced solar radiation scattering by SOA also play a role.*

*Overall, I have a very favorable impression of this conceptual paper and consider it publishable after minor revisions. I do wish, however, that the authors can go beyond the common model validation methods and try to validate the model performance on the ozone-vegetation sensitivity. There are also key details about the model setup that needs to be included in the manuscript. See the comments below.*

**Response:**

Thank you for the helpful comments and suggestions. We have revised the manuscript carefully and the point-to-point responses are listed below.

*Major comments:*

*Section 2.1: What oxidants were considered from the two-product SOA production scheme? If ozone is one of the oxidants considered, is there significant feedback through this pathway (more O3 -> more SOA -> cooling -> reduced isoprene emission) ? The pathway that the authors described was (more isoprene -> more SOA -> cooling -> reduced isoprene emission)*

**Response:**

For the two-product SOA production scheme applied in ModelE2-YIBs, $O_3$ is the only oxidant that considered.

We further examine the feedback of ‘more $O_3$ -> more SOA -> cooling’. Since $O_3$ concentrations are significantly enhanced (more $O_3$) when considering the effect of $O_3$ damage to photosynthesis and stomatal conductance (Fig. 5a and 5b), differences of SOA shortwave radiative forcing between DRY_high or DRY_low and CTRL experiments can be utilized to check whether SOA increases with more $O_3$. As is shown in Fig. R1, the SOA forcing shows very limited changes in eastern China, eastern America, and western Europe, where large $O_3$ enhancements are predicted (Fig. 5a and 5b). Such magnitude is much smaller than that in Fig. 9, which stands for the other pathway (more isoprene -> more SOA -> cooling). As a result, the weaker SOA cooling effect is driven by damaged IPE rather than the enhanced $O_3$ concentrations.

Meanwhile, we did not consider the feedback of SOA cooling on isoprene emissions. Instead, we speculated that weaker SOA cooling (less SOA) promoted temperature and surface $O_3$ concentrations in eastern U.S.

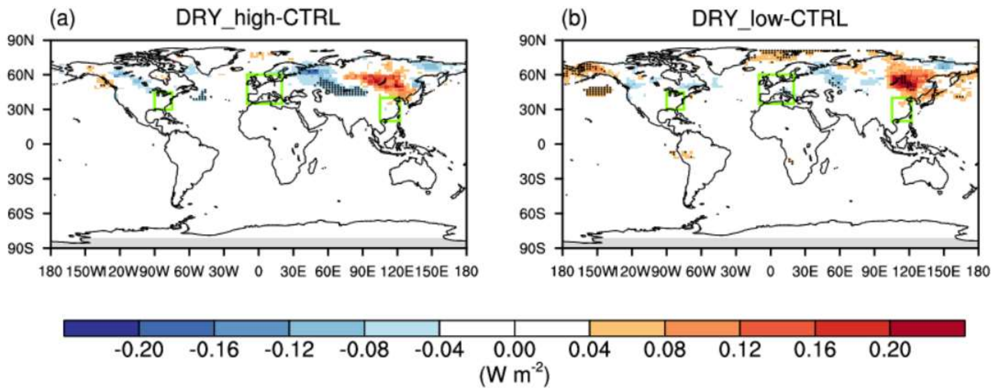

Figure R1. Effects of (a) high and (b) low $O_3$ vegetation damages on SOA shortwave radiative forcing at the surface during the boreal summer. Dotted grids indicate significant changes at the 95% confidence level. Eastern China, eastern U.S. and western Europe are enclosed by green rectangles.

*Section 2.1: What assumptions were made regarding isoprene nitrate formation and its photochemical fate? This has long been shown to significantly impact the response of ozone to isoprene emissions.*

**Response:**

Only three chemical reactions are considered in ModelE2-YIBs related to isoprene:

$$C_5H_8 + OH \rightarrow HCHO + Alkenes$$

$$C_5H_8 + O_3 \rightarrow HCHO + Alkenes$$

$$C_5H_8 + NO_3 \rightarrow HO_2 + Alkenes$$

Both HCHO and $HO_2$ further contribute to the formation of ozone.

The last paragraph of Sect. 2.1 has been revised as:

'Isoprene and α-pinene are considered as the precursors for biogenic secondary organic aerosols (SOA) in ModelE2-YIBs, which are computed online based on the two-product scheme developed by Chung and Seinfeld (2002). Isoprene can be oxidized by $O_3$ as follows:

$$C_5H_8 + O_3 \rightarrow HCHO + A_1P_1 + A_2P_2$$
(5)

Changes for semivolatile product $P_i$ (i=1,2) at each time step ($dt$) are calculated by:

$$\frac{dP_i}{dt} = A_i * rr * [O_3] * [C_5H_8]$$
(6)

where rr is the chemical reaction rate of $O_3$ and isoprene calculated by Arrhenius equation. $[O_3]$ and $[C_5H_8]$ are the $O_3$ and isoprene concentrations, respectively. $A_i$ is the molar based stoicheiometric coefficient depending on SOA formation pathways (high or low $NO_x$) (Lane et al., 2008). Temperature (T) dependence on partitioning coefficient (Kp) for P1 and P2 are given by the Clausius-Clapeyron equation:

$$K_p = K_{sc}\frac{T}{T_{sc}}\exp\left[\frac{\Delta H}{R}\left(\frac{1}{T} - \frac{1}{T_{sc}}\right)\right]$$
(7)

where ΔH is the enthalpy of vaporization and is set as 42.0 kJ $mol^{-1}$ for isoprene (Chung and Seinfeld, 2002;Henze and Seinfeld, 2006) and 72.9 kJ $mol^{-1}$ for α-pinene. Ksc is the saturation concentrations at the temperature Tsc (295 K) and set as 1.62 (0.064) $m^3$ $\mu g^{-1}$ and 0.0086 (0.0026) $m^3$ $\mu g^{-1}$ for the two products formed by oxidation of isoprene (α-pinene), respectively (Presto et al., 2005;Henze and Seinfeld, 2006).' (Page5 Lines 21-31; Page 6 Lines 1-4)

*The validation of the model performance in reproducing surface ozone concentration is unsatisfactory. The model, while no worse than others, does not reproduce well the ozone observations. More importantly, validating the mean surface ozone level does not really give insights to whether the model correctly (or better than other models) reproduces the ozone-vegetation relationship. I wish the authors can make an effort to* *go the extra mile and look at the ozone-temperature dependancy or the ozoneLAI dependency. Also, does the model perform better in the sensitivity simulations including vegetation-chemistry feedbacks?*

**Response:**

Simulated $O_3$ concentrations do show certain biases compared to surface observations. However, if we validate maximum daily 8-hour average (MDA8) [$O_3$], we found that the model shows much lower biases (Fig. S1 in the revised manuscript). The main reason for the overestimation is that the model predicts high nighttime [$O_3$] that are not consistent with observations. Since $O_3$-vegetation interactions usually occur in the daytime, the updated validation shows that ModelE2 is good to use for this study.

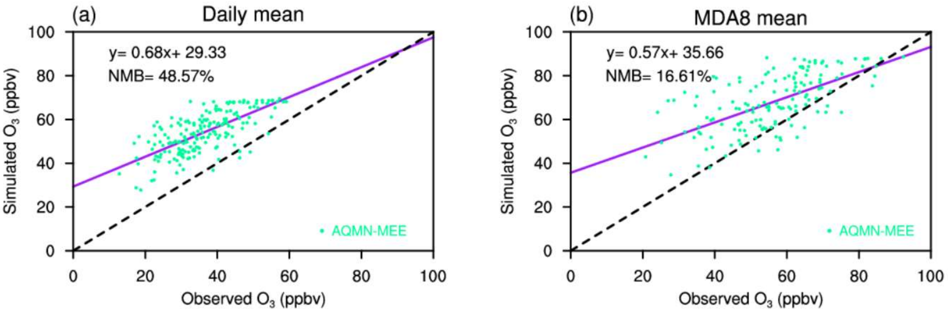

Supplementary Fig. S1. Scatter plots of (a) daily mean and (b) MDA8 $O_3$ concentrations (ppbv) over observational sites in China. The purple line shows the linear regression between the observed and simulated $O_3$ concentrations. The black dashed line shows the 1:1 lines.

Ozone-vegetation relationships have been fully evaluated in our previous studies. For example, we validated $O_3$-GPP relations for six main vegetation types in Yue and Unger (2018) as follows:

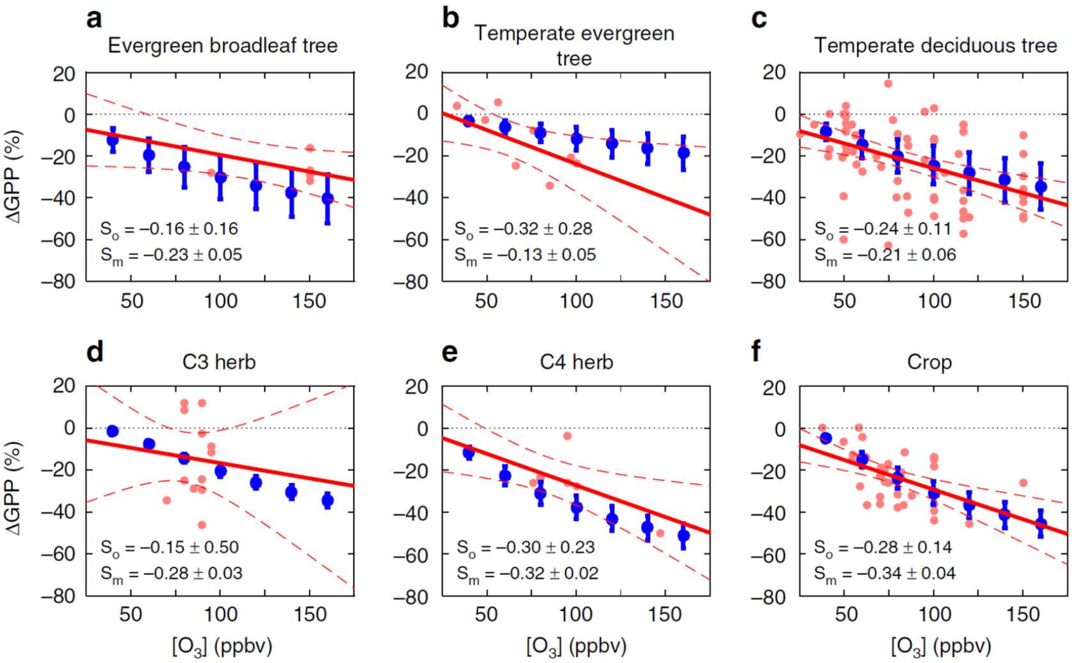

**Figure R2.** Percentage changes in GPP for six main plant functional types (PFTs) caused by $O_3$. Red points on each panel represent literature-based measurements. The linear regression is denoted as a red solid line, with 95% confidence intervals shown as dashed lines. Blue points represent simulated GPP changes from offline sensitivity experiments (Methods), with error bars indicating the range of prediction from low to high $O_3$ damaging sensitivities. The slopes of observed ($S_o$, mean ± 95% confidence interval) and modeled ($S_m$, mean ± (high-low)/2 sensitivity) GPP-$O_3$ sensitivity is shown on each panel (figure from Yue, X., and Unger, N.: Fire air pollution reduces global terrestrial productivity, Nature Communications, 9, 5413, 2018).

We validated $O_3$ damages to stomatal conductance for deciduous trees in Yue et al. (2016) as follows:

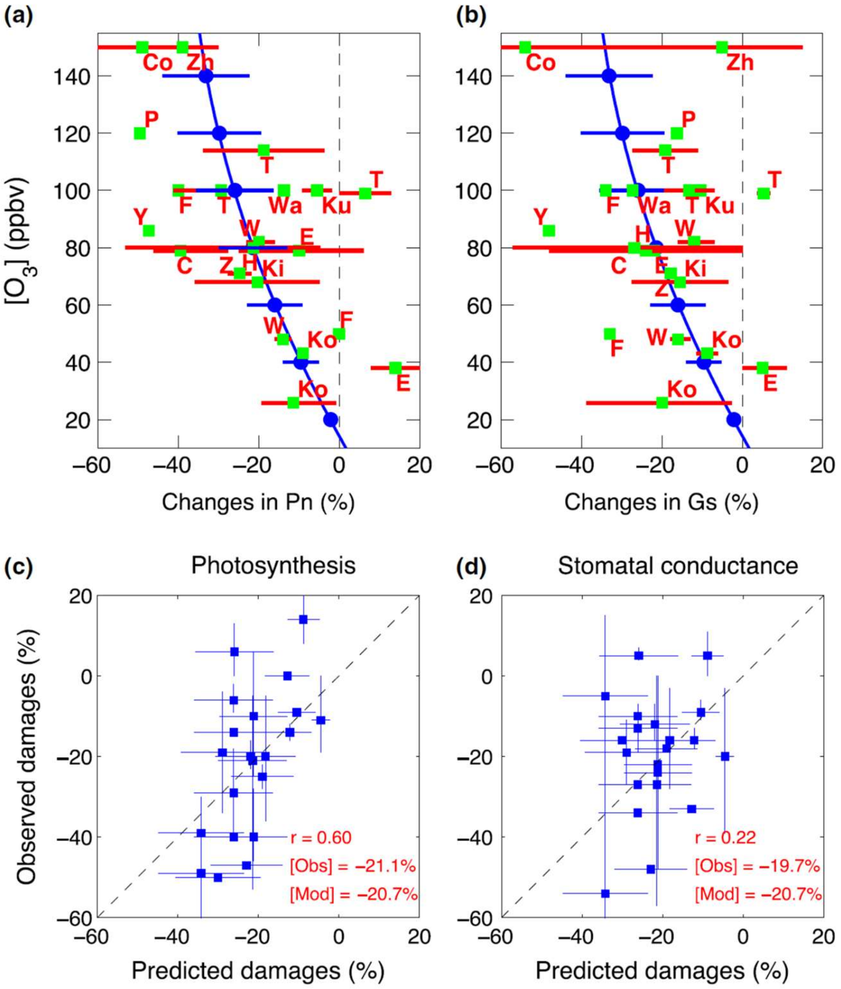

**Figure R3.** Percentage changes in (a) photosynthesis and (b) stomatal conductance averaged across 20 deciduous broadleaf forest flux tower sites in response to different levels of [$O_3$]. The derived percentage changes (including uncertainties) based on the fits are plotted against observations for (c) photosynthesis and (d) stomatal conductance (figure from Yue, X., Keenan, T. F., Munger, W., and Unger, N.: Limited effect of ozone reductions on the 20-year photosynthesis trend at Harvard forest, Global Change Biology, 22, 3750-3759, 2016).

The relations between $O_3$ and LAI can not be evaluated as such observations are not available. However, based on good performance in simulating $O_3$-GPP and GPP-LAI (Yue and Unger, 2015) relationships, we consider ModelE2-YIBs model is appropriate to use for exploring $O_3$-vegetation interactions.

Finally, inclusion of $O_3$-vegetation feedback does not necessarily improve the model performance. The main purpose for this study is to explore the processes and magnitude of $O_3$-vegetation feedback. The positive feedback we revealed may further enhance the model biases, suggesting that additional efforts are required to reduce modeling uncertainties in surface $O_3$.

*The authors suggested that the reason for over-estimation of ozone over China was due to an overestimation of anthropogenic emissions? Is there justification for that? How does the IPCC RCP8.5 emission (van Vuuren et al., 2011) compare to Chinese inventories. The authors also did not mention the basis of their isoprene emission. Have the authors validated their isoprene emissions for the three regions against inversion studies using satellite observations?*

**Response:**

We have revised the first paragraph in Sect. 3.1 as follow:

'Figure 1 shows a comparison of the simulated summer $O_3$ concentrations to the observations. The model in general captures reasonable spatial patterns with a correlation coefficient of 0.41. The NMBs between simulations and observations in U.S and Europe are 11.7% and 13.2%, respectively, which are comparable with the simulation performed by CESM (Lamarque et al., 2012; Sadiq et al., 2017). However, the model overestimates $O_3$ concentrations by 29.3% with a regression intercept of 32 ppbv, suggesting that simulated $O_3$ vegetation damage might be overestimated especially over some regions with low ambient $O_3$ level. The large overestimate is mainly a result of overestimation in China. However, if we validate maximum daily 8-hour average (MDA8) $O_3$ concentrations, we found that the model shows much lower biases (Fig. S1). The main reason for the overestimation is that the model predicts high nighttime $O_3$ concentrations that are not consistent with observations. Since $O_3$-vegetation interactions usually occur in the daytime, the validation shows that ModelE2-YIBs is good to use for this study. Meanwhile, most of the observational sites in AQMN-MEE are located in urban area, which might be another reason for the surface $O_3$ overestimates in China (Yue et al., 2017).' (Page 8, Lines 17-27)

As for the isoprene emissions, extensive validation has been done in previous study (Unger et al., 2013). They showed that a control simulation reproduced 50% of the variability across different ecosystems and seasons in a global database of 28 measured campaign-average fluxes, and captured the observed variance in the 30 min average diurnal cycle ($R^2$ =64–96%) at nine sites. The description of isoprene emissions has been added in the second paragraph in Sect. 2.1:

'…The LAI and tree growth are dynamically simulated with the allocation of carbon assimilation. The emissions of isoprene are calculated online as a function of Je photosynthesis (Eq. 1), canopy temperature, intercellular $CO_2$, and $CO_2$ compensation point (Arneth et al., 2007;Unger, 2013), and have been fully validated by Unger et al. (2013). Carbon fluxes, phenology, LAI, GPP, and net ecosystem exchange (NEE), ….' (Page 5, Lines 1-5)

*Minor comments:*

*Page 4, Lines 23-25: What is the scientific basis for parameterizing stomatal conductance as a function of these parameters, especially A_tot? I realize that a full answer to this question is beyond the scope of this study. Nevertheless, it might worthwhile to say a few words here or in the introduction to justify this assumption, which is central to the results of this study.*

**Response:**

Plant photosynthesis is closely related to stomatal conductance. The higher A_tot requires larger Gs to allow more $CO_2$ enter the leaves for photosynthesis. Such relationship has been parameterized by the Farquhar and Ball-Berry models, which has been widely utilized in land ecosystem simulation (e.g. Farquhar et al., 1980;Ball et al., 1987;Sitch et al., 2007;Bonan et al., 2011;Lombardozzi et al., 2012;Yue and Unger, 2015;Deryng et al., 2016;Sadiq et al., 2017).

The second paragraph of Sect. 2.1 has been revised as:

'The YIBs model is a dynamic vegetation model that includes 9 plant functional types (PFTs) (Table S1) and can simulate biophysical processes of photosynthesis, transpiration and respiration with variations in meteorological fields. **Since the higher leaf photosynthesis requires larger stomatal conductance to allow more $CO_2$ enter the leaves, leaf photosynthesis and stomatal conductance are closely related** and calculated using the Farquhar and Ball–Berry models **(Farquhar et al., 1980;Ball et al., 1987)** as follows:

$$A_{tot} = \min(J_c, J_e, J_s)$$

(1)

$$g_s = m\frac{(A_{tot}-R_d)\times RH}{c_s} + b$$

(2)

where the total leaf photosynthesis ($A_{tot}$) is the minimum value of the ribulose-1,5-bisphosphate carboxylase (RuBisCO)-limited rate of carboxylation ($J_c$), light-limited rate ($J_e$), and export-limited rate ($J_s$). **Stomatal conductance for $H_2O$ ($g_s$)** is calculated by the $A_{tot}$, dark respiration rate ($R_d$), relative humidity ($RH$) and $CO_2$ concentration at the leaf surface ($c_s$). The values of $m$ and $b$ are different for different PFTs (Table S1). A canopy radiation scheme is applied in YIBs to separate diffuse and direct light for sunlit and shaded leaves **(Spitters et al., 1986)**. The LAI and tree growth are dynamically simulated with the allocation of carbon assimilation. Carbon fluxes, phenology, LAI, GPP, and net ecosystem exchange (NEE), as well as other parameters of vegetation in ModelE2-YIBs, have been previously extensively evaluated and agree well with the observations (Yue and Unger, 2015). **In addition, ModelE2-YIBs shows good performance in simulating $O_3$-vegetation interactions such as $O_3$-GPP and $O_3$-$g_s$ relationships (Yue et al., 2016; Yue et al., 2018).**' (Page 4 Lines 21-31; Page 5 Lines 1-7)

*Page 4, Lines 25-26: missing reference for the canopy radiation scheme.*

**Response:**

Revised.

*Page 5, line 12: 'online computed' should be 'computed online'*

**Response:**

Revised.

*Page 5, line 27: How was F_O3 calculated and how was it related to g_s?*

**Response:**

The equation for $F_{O3}$ calculation has been added as follow:

'A semi-mechanistic scheme proposed by Sitch et al. (2007) is applied in this study that simulates the effect of $O_3$ damage to the photosynthesis rate and stomatal conductance via the following formulas:

$$\mathrm{A_{totd}} = \mathrm{F} \times \mathrm{A_{tot}} \tag{8}$$

$$g_{sd} = F \times g_s \tag{9}$$

where $A_{totd}$ ($g_{sd}$) and $A_{tot}$ ($g_s$) are the $O_3$-affected and original total leaf photosynthesis (stomatal conductance), respectively. $F$ is the ratio between affected and original photosynthesis. It depends on the instantaneous leaf uptake of $O_3$ as follows:

$$F = 1 - a \times max\,[F_{O_3} - F_{O_3,crit}, 0.0] \qquad (10)$$

where parameter $a$ represents the $O_3$ damaging sensitivity dependent on vegetation types with a range from low to high values. $F_{O3,crit}$ is a critical threshold for damage (Table S1). $F_{O3}$ is the $O_3$ uptake rate by the stomata, which is calculated by:

$$F_{O3} = \frac{[O_3]}{R_a + [\frac{k_{O3}}{g_{sd}}]} \qquad (11)$$

Where $[O_3]$ is the surface $O_3$ concentrations and $R_a$ is the aerodynamic resistance in Eq. (3). $k_{O3}$ is 1.67, which is the ratio of leaf resistance for $O_3$ to leaf resistance for water vapor. This scheme has been used to explore $O_3$ damages to vegetation in many previous studies…..' (Page 6 Lines 7-19)

*Page 6, line 23: What is n in Equation (10)?*

**Response:**

The Eq. (10) in the origin manuscript and the correspondingly explanation has been revised as:

$$\mathrm{POD_1} = \int_1^n (\mathrm{F_{O_3}} - 1)\mathrm{dt}$$

(14)

'where $F_{O3}$ is the $O_3$ uptake rate by stomata (nmol $O_3$ $m^{-2}$ $s^{-1}$), which is the same as that in Eq. (11). *dt* indicates the time integration step and *n* indicates the total number of time steps during the growing season.' (Page 7 Lines 10-12)

*Figure 1b: Please label the x and y axes. Also, the pastel colors in Figures 1b and S1 are extremely hard to see. Please consider changing the color scheme.*

**Response:**

Revised.

Figure 1:

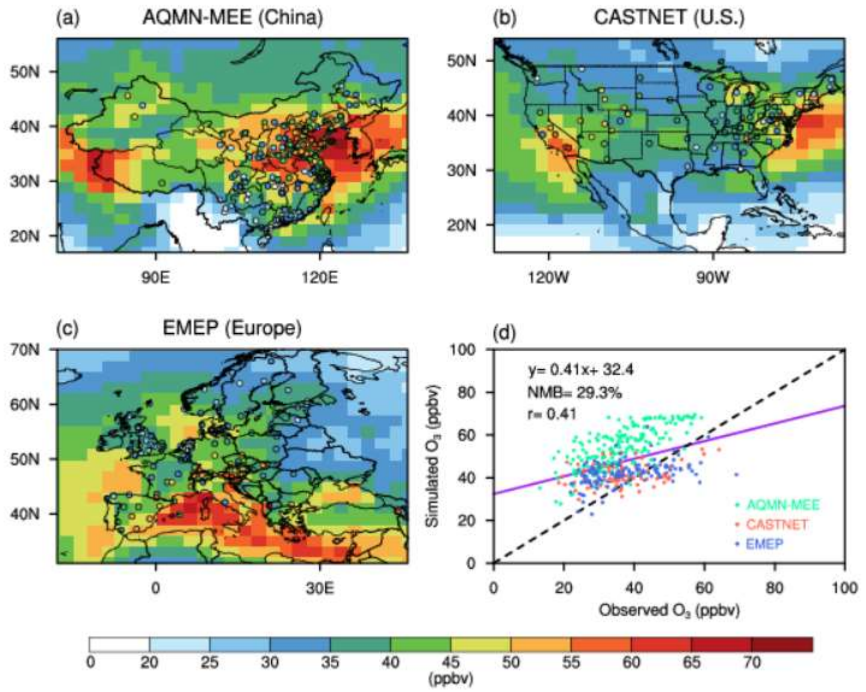

Figure S1 (Figure S2 in the revised manuscript):

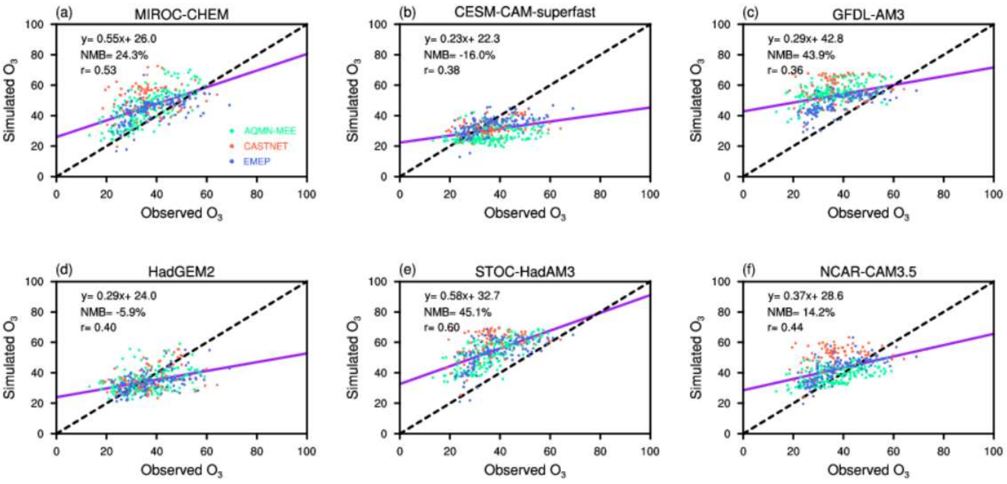

## References

Arneth, A., Niinemets, U., Pressley, S., Back, J., Hari, P., Karl, T., Noe, S., Prentice, I. C., Serca, D., Hickler, T., Wolf, A., and Smith, B.: Process-based estimates of terrestrial ecosystem isoprene emissions: incorporating the effects of a direct CO2-isoprene interaction, Atmospheric Chemistry and Physics, 7, 31-53, 10.5194/acp-7-31-2007, 2007.

Ball, J. T., Woodrow, I. E., and Berry, J. A.: A model predicting stomatal conductance and its contribution to the control of photosynthesis under different environmental conditions, Progress in Photosynthesis Research, 4, 221-224, 1987.

Bonan, G. B., Lawrence, P. J., Oleson, K. W., Levis, S., Jung, M., Reichstein, M., Lawrence, D. M., and Swenson, S. C.: Improving canopy processes in the Community Land Model version 4 (CLM4) using global flux fields empirically inferred from FLUXNET data, Journal of Geophysical Research-Biogeosciences, 116, 10.1029/2010jg001593, 2011.

Chung, S. H., and Seinfeld, J. H.: Global distribution and climate forcing of carbonaceous aerosols, Journal of Geophysical Research-Atmospheres, 107, 10.1029/2001jd001397, 2002.

Deryng, D., Elliott, J., Folberth, C., Mueller, C., Pugh, T. A. M., Boote, K. J., Conway, D., Ruane, A. C., Gerten, D., Jones, J. W., Khabarov, N., Olin, S., Schapho, S., Schmid, E., Yang, H., and Rosenzweig, C.: Regional disparities in the beneficial effects of rising CO2 concentrations on crop water productivity, Nature Climate Change, 6, 786-+, 10.1038/nclimate2995, 2016.

Farquhar, G. D., Caemmerer, S. V., and Berry, J. A.: A BIOCHEMICAL-MODEL OF PHOTOSYNTHETIC CO2 ASSIMILATION IN LEAVES OF C-3 SPECIES, Planta, 149, 78-90, 10.1007/bf00386231, 1980.

Henze, D. K., and Seinfeld, J. H.: Global secondary organic aerosol from isoprene oxidation, Geophysical Research Letters, 33, 10.1029/2006gl025976, 2006.

Lane, T. E., Donahue, N. M., and Pandis, S. N.: Effect of NOx on secondary organic aerosol concentrations, Environmental Science & Technology, 42, 6022-6027, 10.1021/es703225a, 2008.

Lamarque, J. F., Emmons, L. K., Hess, P. G., Kinnison, D. E., Tilmes, S., Vitt, F., Heald, C. L., Holland, E. A., Lauritzen, P. H., Neu, J., Orlando, J. J., Rasch, P. J., and Tyndall, G. K.: CAM-chem: description and evaluation of interactive atmospheric chemistry in the Community Earth System Model, Geoscientific Model Development, 5, 369-411, 10.5194/gmd-5-369-2012, 2012.

Lombardozzi, D., Sparks, J. P., Bonan, G., and Levis, S.: Ozone exposure causes a decoupling of conductance and photosynthesis: implications for the Ball-Berry stomatal conductance model, Oecologia, 169, 651-659, 10.1007/s00442-011-

2242-3, 2012.

Presto, A. A., Hartz, K. E. H., and Donahue, N. M.: Secondary organic aerosol production from terpene ozonolysis. 2. Effect of NOx concentration, Environmental Science & Technology, 39, 7046-7054, 10.1021/es050400s, 2005.

Sadiq, M., Tai, A. P. K., Lombardozzi, D., and Martin, M. V.: Effects of ozone-vegetation coupling on surface ozone air quality via biogeochemical and meteorological feedbacks, Atmospheric Chemistry and Physics, 17, 3055-3066, 10.5194/acp-17-3055-2017, 2017.

Sitch, S., Cox, P. M., Collins, W. J., and Huntingford, C.: Indirect radiative forcing of climate change through ozone effects on the land-carbon sink, Nature, 448, 791-U794, 10.1038/nature06059, 2007.

Spitters, C. J. T., Toussaint, H., and Goudriaan, J.: SEPARATING THE DIFFUSE AND DIRECT COMPONENT OF GLOBAL RADIATION AND ITS IMPLICATIONS FOR MODELING CANOPY PHOTOSYNTHESIS .1. COMPONENTS OF INCOMING RADIATION, Agricultural and Forest Meteorology, 38, 217-229, 10.1016/0168-1923(86)90060-2, 1986.

Unger, N.: Isoprene emission variability through the twentieth century, Journal of Geophysical Research-Atmospheres, 118, 13606-13613, 10.1002/2013jd020978, 2013.

Unger, N., Harper, K., Zheng, Y., Kiang, N. Y., Aleinov, I., Arneth, A., Schurgers, G., Amelynck, C., Goldstein, A., Guenther, A., Heinesch, B., Hewitt, C. N., Karl, T., Laffineur, Q., Langford, B., McKinney, K. A., Misztal, P., Potosnak, M., Rinne, J., Pressley, S., Schoon, N., and Seraca, D.: Photosynthesis-dependent isoprene emission from leaf to planet in a global carbon-chemistry-climate model, Atmospheric Chemistry and Physics, 13, 10243-10269, 10.5194/acp-13-10243-2013, 2013.

Yue, X., and Unger, N.: The Yale Interactive terrestrial Biosphere model version 1.0: description, evaluation and implementation into NASA GISS ModelE2, Geoscientific Model Development, 8, 2399-2417, 10.5194/gmd-8-2399-2015, 2015.

Yue, X., Keenan, T. F., Munger, W., and Unger, N.: Limited effect of ozone reductions on the 20-year photosynthesis trend at Harvard forest, Global Change Biology, 22, 3750-3759, 10.1111/gcb.13300, 2016.

Yue, X., and Unger, N.: Fire air pollution reduces global terrestrial productivity, Nature Communications, 9, 5413, 10.1038/s41467-018-07921-4, 2018.

# Ozone-vegetation feedback through dry deposition and isoprene emissions in a global chemistry-carbon-climate model

Cheng Gong[1, 2], Yadong Lei[2, 3], Yimian Ma[2, 3], Xu Yue[4*] and Hong Liao[4*]

[1]State Key Laboratory of Atmospheric Boundary Layer Physics and Atmospheric Chemistry (LAPC), Institute of Atmospheric Physics, Chinese Academy of Sciences, Beijing, 100029, China

[2]University of Chinese Academy of Sciences, Beijing, 100029, China

[3]Climate Change Research Center, Institute of Atmospheric Physics, Chinese Academy of Sciences, Beijing 100029, China

[4]Jiangsu Key Laboratory of Atmospheric Environment Monitoring and Pollution Control, Jiangsu Collaborative Innovation Center of Atmospheric Environment and Equipment Technology, School of Environmental Science and Engineering, Nanjing University of Information Science and Technology, Nanjing, 210044, China

*Correspondence to*: Xu Yue (yuexu@nuist.edu.cn) and Hong Liao (hongliao@nuist.edu.cn)

**Abstract.** Ozone-vegetation feedback is essential to tropospheric ozone ($O_3$) concentrations. The $O_3$ stomatal uptake damages leaf photosynthesis and stomatal conductance and, in turn, influences $O_3$ dry deposition. Further, $O_3$ directly influences isoprene emissions, an important precursor of $O_3$. The effects of $O_3$ on vegetation further alter local meteorological fields and indirectly influence $O_3$ concentrations. In this study, we apply a fully coupled chemistry-carbon-climate global model (ModelE2-YIBs) to evaluate changes in $O_3$ concentrations caused by $O_3$–vegetation interactions. Different parameterizations and sensitivities of the effect of $O_3$ damage on photosynthesis, stomatal conductance, and isoprene emissions (IPE) are implemented in the model. The results show that $O_3$-induced inhibition of stomatal conductance increases surface $O_3$ on average by +2.1 (+1.4) ppbv in eastern China, +1.6 (-0.5) ppbv in the eastern U.S., and +1.3 (+1.0) ppbv in western Europe at high (low) damage sensitivity. Such positive feedback is dominated by reduced $O_3$ dry deposition, in addition to the increased temperature and decreased relative humidity from weakened transpiration. Including the effect of $O_3$ damage on IPE slightly reduces surface $O_3$ concentrations by influencing precursors. However, the reduced IPE weakens surface shortwave radiative forcing of secondary organic aerosols leading to increased temperature and $O_3$ concentrations in the eastern U.S. This study highlights the importance of interactions between $O_3$ and vegetation with regard to $O_3$ concentrations and the resultant air quality.

## 1 Introduction

Tropospheric ozone ($O_3$) is generated by photochemical reactions involving nitrogen oxides ($NO_x$) and volatile organic compounds (VOCs) under strong solar radiation (Sillman, 1999; Atkinson, 2000; Jacob and Winner, 2009). It is one of the most important air pollutants and has been of widespread concern (Wang et al., 2017; Li et al., 2019). High $O_3$ concentrations at the surface can not only injure human respiratory health (Gauderman et al., 2004; Lelieveld et al., 2015) but also lead to considerable damage to plants and crops, which further changes the land carbon budget (Fuhrer et al., 1997;Yue and Unger, 2014; Lombardozzi et al., 2015). In turn, vegetation can modulate $O_3$ concentrations via influencing dry deposition processes, precursor emissions (such as those of isoprene, monoterpene and sesquiterpene) and meteorological fields. Studying $O_3$–vegetation interactions is of great importance to better understand the variations in $O_3$ concentrations as well as the ecosystem carbon cycle, particularly for regions with high $O_3$ levels and vegetative cover.

Ground-level $O_3$ reduces vegetation photosynthesis by stomatal uptake (Fuhrer et al., 1997; Ainsworth et al., 2012). Through a globally statistical meta-analysis, Wittig et al. (2007) showed that the elevated $O_3$ since the preindustrial period depressed photosynthesis and stomatal conductance of trees by 9-13% and 11-15%, respectively. A recent global meta-analysis on poplar showed that current $O_3$ concentrations reduced the $CO_2$ assimilation rate and stomatal conductance by 33% and 25%, respectively, compared to that of charcoal-filtered air (Feng et al., 2019a). In model studies, an off-line process-based vegetation model (the Yale Interactive Terrestrial Biosphere model, or YIBs) estimated that present-day effect of $O_3$ damage reduced gross primary productivity (GPP) by 4-8% on average over the eastern US during the summer (Yue and Unger, 2014) and annual net primary productivity (NPP) by approximately 14% in China (Yue et al., 2017). Lombardozzi et al. (2015) also showed that the present-day $O_3$ exposure reduces GPP globally by 8–12% using the Community Land Model (CLM).

Isoprene emissions (IPE) from vegetation can be affected by surface $O_3$. Isoprene is the most dominant species among biogenic VOCs (BVOCs) and accounts for approximately one-half of global BVOC emissions (Guenther et al., 2012). The effect of $O_3$ on IPE is complex. Calfapietra et al. (2009) reviewed observational experiments in Italy and proposed a hypothesis that there might be a detoxification effect resulting from $O_3$–IPE interactions. Vegetation under a low accumulated $O_3$ dose can be simulated to increase the levels of IPE to reduce oxidative damage, but months of $O_3$ exposure are harmful to metabolism and reduce IPE. Several studies have showed that $O_3$ fumigation over a short time (days to weeks) but at high concentrations (100-300 ppbv) led to increased IPE (Velikova et al., 2005; Fares et al., 2010), while some other experiments conducted over an entire growing season (at least 3 months) under controlled $O_3$ concentrations (approximately 80 ppbv) showed that $O_3$ reduced IPE (Calfapietra et al., 2008; Yuan et al., 2016; Yuan et al., 2017). A recent global meta-analytic review showed that IPE negatively responded to elevated $O_3$ (91 ppbv on average) by -8% (Feng et al., 2019b). Overall, consecutive exposure to high $O_3$ levels has a negative impact on IPE, although there are large uncertainties resulting from vegetation type (Tiiva et al., 2007; Ryan et al., 2009), temperature (Hartikainen et al., 2009) and $CO_2$ concentration (Calfapietra et al., 2008).

$O_3$ dry deposition is one of the important sink of tropospheric $O_3$ and mainly occurs over vegetation (Wesely, 1989). The stomatal uptake of vegetation plays an important role in this removal process. (Wesely and Hicks, 2000). Val Martin et al.

**Deleted:** Vegetation can affect $O_3$ concentrations through stomatal uptake (the majority of $O_3$ dry deposition).

(2014) showed that the $O_3$ dry deposition velocity in the Community Earth System Model (CESM) significantly increased and was more reasonable when the original scheme (Wesely, 1989), which assumed that stomatal resistance was only related to temperature and water vapor, was replaced with a scheme coupled to vegetation (Collatz et al., 1991; Sellers et al., 1996). In addition, BVOC emissions can change the local $NO_x$/VOC ratio and, in turn, influence $O_3$ concentrations. For example, Fu and Liao (2012) showed that the interannual variations in BVOCs alone can lead to 2-5% differences in simulated $O_3$ over China during the summer using the Model of Emissions of Gases and Aerosols from Nature (MEGAN) (Guenther et al., 2006) module embedded within the global three-dimensional chemical transport model (GEOS-Chem). Calfapietra et al. (2013) reviewed the role of BVOCs emitted by urban trees on $O_3$ concentrations in cities and showed that BVOCs generally promoted $O_3$ formation because of the VOC-limited condition. Furthermore, the modifications of meteorological fields caused by vegetation (Liu et al., 2006; Wu et al., 2011) may also potentially have an effect on $O_3$ formation as well as vegetation growth. As a result, $O_3$ stomatal uptake ($O_3$ dry deposition via stomata), BVOC emissions and changes in meteorological fields are connected and jointly affect $O_3$ concentrations.

Thus far, very few studies have comprehensively investigated the $O_3$-vegetation feedback on a global scale. Sadiq et al. (2017) investigated the effect of $O_3$ damage on the photosynthesis rate and stomatal conductance as well as potential meteorological feedback on surface $O_3$ concentrations using the CESM. They found that $O_3$–vegetation interactions led to increased $O_3$ concentrations mainly in Europe, the northern U.S. and North China. However, the effect of $O_3$ on BVOCs was not directly considered but was indirectly simulated by the increased temperature resulting from $O_3$–vegetation interactions. The $O_3$ damage sensitivities for photosynthesis and stomatal conductance were calculated by using two decoupled linear regressions with accumulated $O_3$ concentrations. However, the linear slope of the photosynthetic rate and stomatal conductance to $O_3$ was zero for some vegetation types (such as broadleaf forests), showing significant effect of $O_3$ damage even at zero $O_3$ concentrations. Based on the same flawed $O_3$ damage scheme, Zhou et al. (2018) calculated responses of leaf area index (LAI) to surface $O_3$ and implemented steady-state results for the GEOS-Chem model to simulate $O_3$ perturbations. Such asynchronous coupling may underestimate $O_3$ changes caused by the full pollution–biosphere interactions, not to mention the omission of feedback of $O_3$ to BVOC emissions and meteorology. More comprehensive work utilizing a validated $O_3$ damage scheme and considering the direct effect of $O_3$ on BVOCs is necessary to reasonably predict $O_3$-vegetation feedback on $O_3$ concentrations.

In this study, we apply a semimechanistic $O_3$ damage scheme (Sitch et al., 2007) to the YIBs dynamic vegetation model coupled with the global Earth system model NASA ModelE2 (ModelE2-YIBs) to explore $O_3$-induced changes in stomatal conductance and evaluate the consequences of such changes on surface $O_3$ concentrations ($O_3$-vegetation feedback via $O_3$ dry deposition). Then, two schemes are proposed to estimate the contributions of $O_3$ damage to IPE based on the existing scheme generated by Sitch et al. (2007), and observations are made. The feedback of $O_3$ damage to both stomatal conductance and IPE and the resultant effect on surface $O_3$ concentrations is calculated by using ModelE2-YIBs. Finally, the associated

**Deleted:** )

**Deleted:** that from

meteorological feedback to $O_3$ concentrations is discussed. We found that the $O_3$-vegetation feedback enhanced surface $O_3$ concentrations particularly in $O_3$-polluted regions.

## 2 Method

### 2.1 The NASA ModelE2-YIBs model

NASA ModelE2-YIBs is a fully coupled chemistry-carbon-climate global model with a horizontal resolution of 2° latitude × 2.5° longitude and 40 vertical layers up to 0.1 hPa. The dynamic and physical processes are calculated every 30 minutes. Gas-phase chemistry in the troposphere includes basic $NO_x$-$HO_x$-$O_x$-CO-$CH_4$ chemistry as well as peroxyacyl nitrates and the following hydrocarbons: terpenes, isoprene, alkyl nitrates, aldehydes, alkenes, and paraffins. Chlorine-containing and bromine-containing compounds, chlorofluorocarbons (CFC) and $N_2O$ source gases are all included in the stratospheric gas-phase chemistry. Dry deposition of gases is calculated by using a resistance-in-series scheme, which was updated to include coupling to stomatal resistance (Val Martin et al., 2014). In addition, the model interactively simulates aerosols such as sulfate, nitrate, elemental and organic carbon, sea salt and dust considering the climate through direct (Koch et al., 2006) and indirect effects (Menon et al., 2008; Menon et al., 2010) and gas-phase chemistry by affecting photolysis rates (Bian et al., 2003). Meteorological and hydrological variables in this model have been fully validated via observations and a reanalysis dataset (Schmidt et al., 2014). The anthropogenic emission inventory for the present-day (2010) from the IPCC RCP8.5 scenario (van Vuuren et al., 2011) is utilized in this study.

The YIBs model is a dynamic vegetation model that includes 9 plant functional types (PFTs) (Table S1) and can simulate biophysical processes of photosynthesis, transpiration and respiration with variations in meteorological fields. Since the higher leaf photosynthesis requires larger stomatal conductance to allow more $CO_2$ enter the leaves, leaf photosynthesis and stomatal conductance are closely related and calculated using the Farquhar and Ball–Berry models (Farquhar et al., 1980; Ball et al., 1987) as follows:

**Deleted:** Leaf

**Deleted:** by

$$A_{tot} = \min(J_c, J_e, J_s) \tag{1}$$

$$g_s = m\frac{(A_{tot} - R_d) \times RH}{c_s} + b \tag{2}$$

where the total leaf photosynthesis ($A_{tot}$) is the minimum value of the ribulose-1,5-bisphosphate carboxylase (RuBisCO)-limited rate of carboxylation ($J_c$), light-limited rate ($J_e$), and export-limited rate ($J_s$). Stomatal conductance for $H_2O$ ($g_s$) is calculated by the $A_{tot}$, dark respiration rate ($R_d$), relative humidity ($RH$) and $CO_2$ concentration at the leaf surface ($c_s$). The values of $m$ and $b$ are different for different PFTs (Table S1). A canopy radiation scheme is applied in YIBs to separate diffuse and direct light for sunlit and shaded leaves (Spitters et al., 1986). The LAI and tree growth are dynamically simulated with the allocation of carbon assimilation. The emissions of isoprene are calculated online as a function of *Je* photosynthesis (Eq. (1)), canopy temperature, intercellular $CO_2$, and $CO_2$ compensation point (Arneth et al., 2007;Unger, 2013), and have been

**Deleted:** .

fully validated by Unger et al. (2013). Carbon fluxes, phenology, LAI, GPP, and net ecosystem exchange (NEE), as well as other parameters of vegetation in ModelE2-YIBs, have been previously extensively evaluated and agree well with the observations (Yue and Unger, 2015). In addition, ModelE2-YIBs shows good performance in simulating $O_3$-vegetation interactions such as $O_3$-GPP and $O_3$-$g_s$ relationships (Yue et al., 2016; Yue et al., 2018).

The $O_3$ dry deposition velocity ($V_d$) in ModelE2-YIBS are calculated following the multiple-resistance approach originally described by Wesely (1989):

$$V_d = \frac{1}{R_a+R_b+R_c} \qquad (3)$$

where $R_a$, $R_b$ and $R_c$ are the aerodynamic resistance, quasi-laminar sublayer resistance above canopy, and surface resistance, respectively. $R_c$ is computed as follows:

$$\frac{1}{R_c} = \frac{1}{R_s} + \frac{1}{R_{lu}} + \frac{1}{R_{cl}} + \frac{1}{R_g} \qquad (4)$$

where $R_s$, $R_{lu}$, $R_{cl}$ and $R_g$ represent the stomatal resistance, leaf cuticle resistance, lower canopy resistance and the ground resistance, respectively. In this study, the original parameterization for $R_s$, which is empirically expressed by solar radiation, surface air temperature, and the molecular diffusivities for water vapor, has been substituted by the reciprocal of $g_s$ from Eq. (2) following Val Martin et al. (2014). In this case, $O_3$ dry deposition can be interactively influenced by the stomatal $O_3$ uptake process for vegetation.

Isoprene and α-pinene are considered as the precursors for biogenic secondary organic aerosols (SOA) in ModelE2-YIBs, which are computed online based on the two-product scheme developed by Chung and Seinfeld (2002). Isoprene can be oxidized by $O_3$ as follows:

$$C_5H_8 + O_3 \rightarrow HCHO + A_1P_1 + A_2P_2 \qquad (5)$$

Changes for semivolatile product $P_i$ (i=1,2) at each time step ($dt$) are calculated by:

$$\frac{dP_i}{dt} = A_i * rr * [O_3] * [C_5H_8] \qquad (6)$$

where rr is the chemical reaction rate of $O_3$ and isoprene calculated by Arrhenius equation. $[O_3]$ and $[C_5H_8]$ are the $O_3$ and isoprene concentrations, respectively. $A_i$ is the molar based stoicheiometric coefficient depending on SOA formation pathways (high or low $NO_x$) (Lane et al., 2008). Temperature ($T$) dependence on partitioning coefficient ($K_p$) are given by the Clausius-Clapeyron equation:

$$K_p = K_{sc}\frac{T}{T_{sc}}exp\left[\frac{\Delta H}{R}\left(\frac{1}{T}-\frac{1}{T_{sc}}\right)\right] \qquad (7)$$

where ΔH is the enthalpy of vaporization and is set as 42.0 kJ $mol^{-1}$ for isoprene (Chung and Seinfeld, 2002; Henze and Seinfeld, 2006) and 72.9 kJ $mol^{-1}$ for α-pinene. $K_{sc}$ is the saturation concentrations at the temperature $T_{sc}$ (295 K) and set as

**Deleted:** YIBs

**Deleted:** online

**Deleted:** . The mass-based yields of semivolatile species are set following Presto et al. (2005). Temperature ($T$) dependence on partitioning coefficient ($K_p$) are given by the Clausiuse-Clapeyron equation:¶

**Deleted:** (5

1.62 (0.064) $m^3$ $\mu g^{-1}$ and 0.0086 (0.0026) $m^3$ $\mu g^{-1}$ for the two products formed by oxidation of isoprene (α-pinene), respectively (Presto et al., 2005; Henze and Seinfeld, 2006).

### 2.2 Schemes describing the effect of $O_3$ damage to vegetation

### 2.2.1 The effect of $O_3$ damage to photosynthesis and stomatal conductance

A semi-mechanistic scheme proposed by Sitch et al. (2007) is applied in this study that simulates the effect of $O_3$ damage to the photosynthesis rate via the following formula:

$$A_{totd} = F \times A_{tot} \quad (8)$$

$$g_{sd} = F \times g_s \quad (9)$$

where $A_{totd}$ ($g_{sd}$) and $A_{tot}$ ($g_s$) are the $O_3$-affected and original total leaf photosynthesis (stomatal conductance), respectively. $F$ is the ratio between affected and original photosynthesis. It depends on the instantaneous leaf uptake of $O_3$ as follows:

$$F = 1 - a \times max\,[F_{O_3} - F_{O_3,crit}, 0.0] \quad (10)$$

where parameter $a$ represents the $O_3$ damaging sensitivity dependent on vegetation types with a range from low to high values. $F_{O3,crit}$ is a critical threshold for damage (Table S1). $F_{O3}$ is the $O_3$ uptake rate by the stomata, which is calculated by:

$$F_{O3} = \frac{[O_3]}{R_a + [\frac{k_{O3}}{g_{sd}}]} \quad (11)$$

where $[O_3]$ is the surface $O_3$ concentrations and $R_a$ is the aerodynamic resistance in Eq. (3). $k_{O3}$ is 1.67, which is the ratio of leaf resistance for $O_3$ to leaf resistance for water vapor. This scheme has been utilized in many previous studies, which have reported that $O_3$ reduces GPP by 4–8% on an annual mean basis in the eastern U.S. and by 10-20% during the summer in China (Yue and Unger, 2014; Yue et al., 2017).

### 2.2.2 The effect of $O_3$ damage to IPE

To date, there are no mature parameterizations that calculate the contributions of $O_3$ damage to IPE. Here, we propose two schemes based on observations to quantify the changes in surface $O_3$ concentrations resulting from $O_3$ damage to IPE.

The first scheme assumes that $O_3$ leads to the same percentage of damage to photosynthesis and IPE because IPE are observed to linearly vary with photosynthesis (Yuan et al., 2016). The affected IPE ($IPE_d$) can be calculated as follows:

$$IPE_d = F \times IPE \quad (12)$$

where F is calculated by using Eq. (10) and $IPE$ is the original level of IPE. Hereafter, this scheme is termed the "F scheme."

Another scheme is based on open-top chamber (OTC) observations. Although many experiments have studied the effects of $O_3$ on IPE, most have applied a limited range of $O_3$ levels (e.g., 7.3-56.6 ppbv in Hartikainen et al. (2009) or >100 ppbv in Fares et al., (2010)). In reality, surface $O_3$ concentrations can vary from several parts-per-billion-volume (e.g., in the polar

**Deleted:** semi-mechanistic

**Deleted:** 6

**Deleted:** damaged

**Deleted:** ,

**Deleted:** ,

**Deleted:** $F$ is an "uptake of $O_3$ factor" depending

**Deleted:** max

**Deleted:** 7

**Deleted:** $F_{O3}$ is the $O_3$ uptake rate by the stomata and $F_{O3,crit}$ is the critical vegetation-

**Deleted:** threshold for damage. Parameter $a$ has two series of values for different

**Deleted:** representing high or

**Deleted:** sensitivities

**Deleted:** $O_3$

**Moved (insertion) [1]**

**Deleted:** Moreover, damaged photosynthesis leads to a lower stomatal conductance via formula (2) to aid vegetation

**Deleted:** to potential $O_3$ damage

**Deleted:** A photosynthesis-based scheme is applied in the model to simulate IPE, which is the function of the $J_e$, canopy temperature and intercellular $CO_2$ concentration (Arneth et al., 2007; Unger, 2013).…

**Deleted:** 8

**Deleted:** 7

region during the winter) to over 100 ppbv (e.g., in megacities of China during the summer). To date, only one study (Yuan et al., 2017) has explored the responses of IPE to different levels of $O_3$ damage for two poplar clones; a linear regression between the percentage damage of IPE (*PDI*) and the cumulative stomatal uptake of $O_3$ > 1 nmol $O_3$ $m^{-2}$ $s^{-1}$ ($POD_1$) was derived as follows:

$$\mathrm{PDI} = (-0.0086 \times POD_1 + 1.0194) \times 100 \qquad (13)$$

The $POD_1$ is calculated by the following formula:

$$\mathrm{POD_1} = \int_1^n (\mathrm{F_{O_3}} - 1)\mathrm{dt} \qquad (14)$$

where $F_{O3}$ is the $O_3$ uptake rate by stomata (nmol $O_3$ $m^{-2}$ $s^{-1}$), which is the same as that in Eq. (11). *dt* indicates the time integration step and *n* indicates the total number of time steps during the growing season. In this study, the $POD_1$ accumulated over the growth season, which is defined as April to October north of 23.5°N (e.g., Tucker et al., 2001; White et al., 2002; Yin et al., 2014; Wang et al., 2019), November to March south of 23.5°S (e.g., Broich et al., 2015; Moore et al., 2016), and 200 days between 23.5°N to 23.5°S because the leaf phenology in tropical evergreen forests is not determined by seasonality (Xiao et al., 2006). Limited by the data availability, we apply the PDI function (Eq. (13)) for poplar to all vegetation types as follow:

$$IPE_d = \min\,(PDI, 100\%) \times IPE \qquad (15)$$

Hereafter, this scheme is termed a "linear scheme." Different from the F scheme, the linear scheme calculates IPE damage using accumulated $O_3$ instead of instantaneous $O_3$ concentrations.

### 2.3 Descriptions for sensitivity experiments

Seven experiments (Table 1) are conducted to explore the feedback of vegetation on surface $O_3$ concentrations via influencing $O_3$ dry deposition, IPE, as well as meteorological fields. The control simulation (CTRL) does not include the effect of $O_3$ damage to vegetation. Two cases (DRY_high and DRY_low) are established to investigate the feedback via $O_3$ dry deposition with high or low $O_3$ damage sensitivities (*a* in Eq. (10)). Then, the effect of $O_3$ damage to IPE is added by using either F or linear schemes, resulting in four more experiments (TOTAL_F_high, TOTAL_F_low, TOTAL_LINEAR_high, and TOTAL_LINEAR_low). In the CTRL run, the effects of $O_3$ damage to photosynthesis, stomatal conductance, and IPE (the linear scheme) are calculated offline; such damages are not fed back to affect vegetation growth and dry deposition of $O_3$. The offline $O_3$ damage to IPE produced by using the F scheme is calculated in DYR_high and DYR_low.

For each experiment, 20-year simulations are performed with 5 initial spin-up years. Outputs of the last 15 years are averaged and analyzed. Regionally, the results in the eastern U.S. (30°N-45°N, 75°W-90°W), western Europe (35°N-60°N, 10°W-20°E) and eastern China (20°N-40°N, 105°E-122°E) are compared and discussed.

**Deleted:** $POD_1 = \int_{i=1}^{n} (F_{O_3} - 1)dt$ (10)¶

**Deleted:** (7).

**Deleted:** We

**Deleted:** same

**Deleted:** 9)) of

**Deleted:** for

**Deleted:** because of the data limit

**Deleted:** follows

**Moved up [1]:** (11)¶

**Deleted:** 7

**Deleted:** offline

**Deleted:** and

**Deleted:** are calculated using the Sitch et al. (2007) scheme; offline $O_3$ damage to

**Deleted:** is calculated using

**Deleted:** .

**Deleted:** For these offline simulations, $O_3$-induced damage is not fed back to affect the climate, chemistry, or carbon cycle.

### 2.4 Observed ground-level $O_3$ network and model evaluation

To evaluate simulated $O_3$ concentrations, three observational networks are utilized as follows: the Air Quality Monitoring Network from Ministry of Ecology and Environment (AQMN-MEE) in China, Clean Air Status and Trends Network (CASTNET) in the U.S. and European Monitoring and Evaluation Programme (EMEP) in Europe. The summer concentrations for CASTNET and EMEP are averaged over the year 2010 but those for AQMN-MEE are averaged over 2014 because this network was established in 2013 and started to provide high-quality data beginning in 2014. The simulated $O_3$ concentrations are interpolated in the observational sites by using a bilinear interpolation method. Normalized mean biases (NMBs) are calculated by using the following equation:

$$\mathrm{NMB} = \sum_{i}^{n}(S_i - O_i) \, / \sum_{i}^{n} O_i * 100\% \qquad (16)$$

where $S_i$ and $O_i$ are the simulated and observed $O_3$ concentrations, respectively, and $n$ is the total number of observational sites.

## 3 Results

### 3.1 CTRL simulation and model evaluation

Figure 1 shows a comparison of the simulated summer $O_3$ concentrations to the observations. The model in general captures reasonable spatial patterns with a correlation coefficient of 0.41. The NMBs between simulations and observations in U.S and Europe are 11.7% and 13.2%, respectively, which are comparable with the simulation performed by CESM (Lamarque et al., 2012; Sadiq et al., 2017). However, the model overestimates $O_3$ concentrations by 29.3% with a regression intercept of 32 ppbv, suggesting that simulated $O_3$ vegetation damage might be overestimated especially over some regions with low ambient $O_3$ level. The large overestimate is mainly a result of overestimation in China. However, if we validate maximum daily 8-hour average (MDA8) $O_3$ concentrations, we found that the model shows much lower biases (Fig. S1). The main reason for the overestimation is that the model predicts high nighttime $O_3$ concentrations that are not consistent with observations. Since $O_3$-vegetation interactions usually occur in the daytime, the validation shows that ModelE2-YIBs is good to use for this study. Meanwhile, most of the observational sites in AQMN-MEE are located in urban area, which might be another reason for the surface $O_3$ overestimates in China (Yue et al., 2017).

To further compare the performance of ModelE2-YIBS with other chemistry-climate models, we select six simulated cases performed by different model members in Atmospheric Chemistry and Climate Model Intercomparision Project (ACCMIP) (Lamarque et al., 2013) and implement the evaluation with the same observational data (Fig. S2). The correlation coefficient (0.41) and NMB (29.3%) for ModelE2-YIBs are located in the ranges of 0.36 to 0.60 and -16.0% to 45.1% by the model ensembles, suggesting that ModelE2-YIBS has comparable performance with other state-of-the-art models. However, most of the current chemistry-climate models lack the interactive vegetation growth module, let alone studying $O_3$-vegetation

**Deleted:** 12

**Deleted:** , although it overestimates $O_3$ concentrations by 29.3%.

**Deleted:** NMB

**Deleted:** is

**Deleted:** is

**Deleted:** (Lamarque et al., 2012; Sadiq et al., 2017).

**Deleted:** , where the anthropogenic emissions has been rapidly changing in recent years (Zheng et al., 2018). As a result, the surface

**Deleted:** may show large differences between

**Deleted:** year of 2010 and 2014. Also, the rural

**Deleted:** are likely higher than urban $O_3$ concentrations because of

**Deleted:** $NO_x$ titration effect in cities. However

**Deleted:** (Yue et al., 2017).

**Deleted:** YIBs

**Deleted:** S1

**Deleted:** within

**Deleted:** YIBs

**Deleted:** coupling between

**Deleted:** and chemistry, which is the main focus of this study interactions. The vegetation variables (e.g. GPP and LAI) in ModelE2-YIBs have been fully evaluated in previous studies (Yue and Unger, 2015), making ModelE2-YIBs a suitable tool for this work.

Figure 2 shows the global June-July-August (JJA) surface $O_3$ concentrations, $O_3$ dry deposition velocity, GPP and IPE. Simulated $O_3$ is high in the eastern U.S., western Europe, India, and eastern China (Fig. 2a). The spatial pattern of $O_3$ dry deposition velocity (Fig. 2b) resembles that of the GPP (Fig. 2c) because the $O_3$ stomatal uptake dominantly contributed to the dry deposition. Both are high in the eastern U.S., western Europe, Amazon, eastern China, and Indonesia and show a reasonable magnitude consistent with previous modeling studies (Val Martin et al., 2014; Yue and Unger, 2015; Sadiq et al., 2017). The spatial pattern of IPE (Fig. 2d) also resembles that of the GPP (Fig. 2c), except that the IPE in Europe are lower than those in other regions. Such discrepancies are likely attributed to the lower fraction of deciduous broadleaf forest, which provides a high yield of IPE (Potter et al., 2001).

### 3.2 Offline $O_3$ damage to IPE

Figure 3 shows the effect of $O_3$ damage to IPE during the boreal summer. For different schemes, reductions in IPE show a similar spatial distribution with significant damages in the eastern U.S., western Europe, and eastern China, where both $O_3$ concentrations and vegetative cover are high. For the F scheme with high sensitivity, the damage mediated by the IPE can reach as high as 30% in eastern China and > 20% in the eastern U.S. and western Europe (Fig. 3a). However, the F scheme with low sensitivity predicts a low damage of ~10% in these regions (Fig. 3b). On a global scale, IPE decreases by 1.2-3.2% because of the $O_3$ effect. The damage using the linear scheme is generally within the low-to-high range of predictions by using the F schemes. For the linear scheme, IPE in eastern China show the greatest damage of ~15%.

Figure 4 shows seasonal variations in the effect of $O_3$ damage to IPE in eastern China, the eastern U.S. and western Europe. The magnitude of IPE changes is generally within the range of 10-29%, as summarized by the observational meta-analysis (Feng et al., 2019b). The F scheme is dependent on instantaneous $O_3$ uptake, which peaks during the summer when both surface $O_3$ and stomatal conductance are high. In contrast, the linear scheme depends on the accumulated $O_3$ flux, which increases from zero to high levels during the growth season. As shown, the percentage of $O_3$ damage to IPE is low during April and May but increases to a similar magnitude as that in the F scheme with high sensitivity during August; it reaches a maximum in October. The differences in the F (instantaneous) and linear (accumulated) schemes cause distinct seasonal variations in the IPE damage, which might cause different feedback to the $O_3$ concentrations. However, the IPE peaks during summer (Fig. S3), suggesting that absolute changes in IPE are most significant during this season (Fig. S4). Meanwhile, since the surface $O_3$ concentrations and the vegetation growth both peak during boreal summer in northern hemisphere, the $O_3$-vegetation

**Deleted:** is

**Deleted:** S2

interactions are supposed to be the strongest in this season. As a result, we focus our analyses on the summer to explore the $O_3$-vegetation interactions and feedback.

### 3.3 $O_3$-vegetation feedbacks on surface $O_3$ concentrations

The effect of $O_3$ damage to stomatal conductance inhibits dry deposition (Fig. S5) leading to significant increases in summer surface $O_3$, particularly in eastern China, Japan, the eastern U.S., and western Europe (Figs. 5a-b). The positive feedback can be greater than 5 ppbv in eastern China with high sensitivity (Fig. 5a). Smaller changes are predicted for low sensitivity, which shows limited perturbations in the U.S. and Japan (Fig. 5b). Including the effect of $O_3$ damage to both stomatal conductance and IPE maintains the spatial pattern of $O_3$ changes but occurs at a lower magnitude (Figs. 5c-f) because these two effects offset each other. With high damage to stomatal conductance, surface $O_3$ remains increasing in eastern China, Japan, the eastern U.S., and western Europe even with reduced IPE (Figs. 5c and 5e). However, with low damage to stomatal conductance, surface $O_3$ shows limited changes in Europe, China and Japan when IPE are simultaneously reduced (Figs. 5d and 5f). Surprisingly, surface $O_3$ increases over the eastern U.S. in these cases (Figs. 5d and 5f) compared to the limited changes when IPE remain unperturbed (Fig. 5b).

**Deleted:** S3

Figure 6 summarizes the changes in surface $O_3$ over sensitive regions. Without IPE feedback, the effect of $O_3$ damage to stomatal conductance leads to changes in regionally averaged surface $O_3$ by +2.1 (+1.4) ppbv in eastern China, +1.6 (-0.5) ppbv in the eastern U.S., and +1.3 (+1.0) ppbv in western Europe for high (low) damage sensitivity. Changes in eastern China are the greatest compared to those of the other two regions, mainly because of the high $O_3$ level (Fig. 1a) and sensitive tree species (the high $a$ and low $F_{o3,crit}$ for deciduous broadleaf forest, Table S1). Surface $O_3$ is predicted to decrease in the eastern U.S. with the low damage sensitivity, though such a change is not significant over most grids (Fig. 5b). The inclusion of the effect of $O_3$ damage for both stomatal conductance and IPE slightly weakens the $O_3$ feedback, leading to changes in $O_3$ concentrations of +1.7 (+0.4) ppbv with the F scheme and +2.1 (-0.1) ppbv with the linear scheme in eastern China for high (low) sensitivity. The regional maximum $O_3$ changes can reach 6.9 (3.9) ppbv in eastern China. Further, the effect of $O_3$ damage to IPE weakens the positive feedback in western Europe by approximately 1-2 ppbv. The negative $O_3$ changes in the eastern U.S. with low $O_3$ damage are +0.9 (F scheme) or +0.8 (linear scheme) ppbv on average when IPE feedback is included.

Although damage to stomatal conductance and IPE exert opposite effects, surface $O_3$ in general increases after including both processes (Fig. 6), suggesting that dry deposition inhibition plays the dominant role. For the same $O_3$ damage sensitivity to stomatal conductance, changes in surface $O_3$ remain similar over eastern China and the eastern U.S. between the F and linear schemes in terms of the responses of the IPE. However, responses in western Europe are weaker for the linear scheme (Fig. 5e) compared to that of the F scheme (Fig. 5c), though the former predicts lower reductions in IPE (Fig. 3). Nevertheless, inclusion of IPE reductions helps increase surface $O_3$ over the eastern U.S. (Figs. 5d/5f vs. Fig. 5b), which is unexpected since

**Deleted:** ).

the reduction in IPE is supposed to decrease $O_3$ concentrations. These changes are speculated to be indirectly related to $O_3$-vegetation feedback to meteorology and would be further examined in the next section.

**Deleted:** cannot be explained by the changes in IPE but

**Deleted:** $O_3$

### 3.4 Effects of $O_3$–vegetation interactions on meteorology and vegetation

Figure 7 and Figure 8 show the changes in surface air temperature and relative humidity (RH) between different sensitivity experiments and the CTRL simulation, respectively. When considering the effect of $O_3$ damage to stomatal conductance alone, eastern China becomes warmer (Fig.7a and 7b) and drier (Fig.8a and 8b), favoring $O_3$ chemical production and increasing surface $O_3$ concentrations (Jacob and Winner, 2009). The damaged stomatal conductance weakens leaf-level transpiration and thus reduces the latent heat flux at the surface (Fig. S6), leading to a higher temperature and lower RH. The effect of $O_3$ damages are weaker in the eastern U.S. and western Europe because of the lower $O_3$ concentrations, resulting in insignificant changes in temperature and RH over these regions.

**Deleted:** S4

**Deleted:** the

The effect of $O_3$ damage to IPE has limited impacts on RH (as shown in Figs. 8c/e vs. 8a and Figs. 8d/f vs. 8b) but significantly increases surface air temperature in the eastern U.S. (as shown in Figs. 7c/e vs. 7a and Figs. 7d/f vs. 7b). The temperature in western Europe also slightly increases when IPE reductions are included, particularly when utilizing the F scheme with high sensitivity (Fig. 7c). Isoprene is among the most important precursors for the formation of secondary organic aerosols (SOAs) (Claeys et al., 2004), which are able to reduce surface air temperature by light extinction (Charlson et al., 1992). As a result, the $O_3$-induced reduction of IPE decreases SOA loading and weakens the “cooling effect” of aerosols, leading to a higher temperature at the surface. The positive changes in shortwave radiative forcing following SOA reduction are the strongest in the eastern U.S. when considering the effect of $O_3$ damage to IPE, particularly for the F schemes with high sensitivity (Fig. 9). Such warming explains why the reduced IPE helps increase the surface $O_3$ in the eastern U.S. (Fig. 6). However, aerosols in regions with high anthropogenic emissions (such as eastern China) are more dominated by inorganic components (Sun et al., 2006; Yang et al., 2011); thus, the changes in SOAs are less important. As a result, the feedback of $O_3$-induced IPE reductions on temperature is not significant in eastern China compared to that of other regions.

In addition to the direct damage (Fig. 3), IPE are indirectly affected by perturbations in the LAI and meteorology. Figure S5 shows that the LAI decreases in three polluted regions (eastern China, the eastern U.S. and western Europe) because of the $O_3$-mediated inhibition of photosynthesis, although the magnitude is typically within 5%. Moderate changes in the LAI by $O_3$ have also been reported in previous studies (Yue and Unger, 2015; Sadiq et al., 2017), suggesting that LAI feedback is too low to effectively influence IPE and the consequent surface $O_3$. Furthermore, the warming effects resulting from the $O_3$-induced inhibition on stomatal conductance (Fig. 7) and the changes in the LAI (Fig. S7) cause limited changes in IPE (Fig. S8), suggesting that $O_3$-vegetation feedback does not significantly change IPE. In comparison, Sadiq et al. (2017) reported a strong positive feedback (3-5 times greater than our results) on IPE caused by increased temperature from reduced transpiration when

**Deleted:** S6

the effect of $O_3$ damage to stomatal conductance is considered. However, Sadiq et al. (2017) might have overestimated temperature feedback because their parameterizations of $O_3$ damage to plants employ constant intercepts for some PFTs, which results in sustained damage even at low $O_3$ concentrations.

## 4 Conclusions and discussion

In this study, we explore the effect of $O_3$-vegetation feedback on surface $O_3$ concentrations by considering the effects of $O_3$ damage on photosynthesis, stomatal conductance, and IPE in a fully coupled global chemistry-carbon-climate model. Three regions with high $O_3$ levels and dense vegetation cover, including eastern China, the eastern U.S. and western Europe, are examined during the summer. The positive feedback increases $O_3$ concentrations on average by +2.1 (+1.4) ppbv in eastern China, +1.6 (-0.5) ppbv in the eastern U.S., and +1.3 (+1.0) ppbv in western Europe for high (low) $O_3$ damage to stomatal conductance and the consequent inhibition of dry deposition. Additionally, the effect of $O_3$ damage to stomatal conductance increases the surface temperature and decreases the RH by weakening transpiration, which favors $O_3$ chemical production and increases surface $O_3$ concentrations. Including the effect of $O_3$ damage to IPE slightly weakens the positive feedback in eastern China and western Europe but increases $O_3$ concentrations by 0.9-1.5 ppbv with the F scheme or 0.8-1.2 ppbv with the linear scheme in the eastern U.S. The increased temperature following reduced SOA concentrations are speculated as a possible cause for this result. Our results show that $O_3$–vegetation interactions increase surface $O_3$ by reducing dry deposition (from inhibition of stomatal conductance) and increasing chemical formation (from surface warming by weakening transpiration and SOA radiative forcing). However, changes in precursor IPE as well as the LAI have limited impacts on surface $O_3$.

**Deleted:** main cause for this result is likely related to the

Sadiq et al. (2017) also showed positive $O_3$-vegetation feedback on the surface $O_3$ in a global model. Compared to their results, we find an ultimate positive feedback with similar magnitude of surface $O_3$ concentrations but different spatial pattern. The strongest feedback in eastern China rather than western Europe, which is more reasonable, as the $O_3$ level in China is much higher than that in Europe (Lu et al., 2018). In addition, the effect of $O_3$-vegetation feedback on temperature is lower in our study. The fixed decoupled scheme in Sadiq et al. (2017) may have overestimated the effect of $O_3$ damage to stomatal conductance, leading to stronger feedback on $O_3$ concentrations and temperature. Furthermore, the mechanisms of $O_3$ effects on IPE are different. Sadiq et al. (2017) showed increased IPE because of the warming feedback. However, such warming is not significant in our study (Fig. S8). Instead, we include direct effect of $O_3$ damage to IPE based on observations. Although the simulations show limited impacts of reduced IPE on surface $O_3$, the simultaneously reduced SOAs contribute to increased surface $O_3$ by weakening shortwave radiative forcing and increasing temperature in the eastern U.S.

**Deleted:** show the

**Deleted:** S6

Our results are subject to uncertainties in modeled $O_3$ and damaging schemes. ModelE2-YIBs overestimates summer $O_3$, particularly in China (Fig. 1), which may exacerbate the damage to stomatal conductance and the consequent feedback. The

$O_3$ damage parameterization by Sitch et al. (2007) is a semiphysical scheme that couples photosynthesis and stomatal conductance. However, some observational studies have showed that the sluggish stomatal responses under chronic $O_3$ exposure lead to stomata losing function and decoupling from photosynthesis (Paoletti and Grulke, 2005; Gregg et al., 2006). The decoupled parameterization proposed by Lombardozzi et al. (2012) has been applied to estimate the effect of $O_3$ damage to photosynthesis and stomatal conductance (Lombardozzi et al., 2015; Sadiq et al., 2017; Zhou et al., 2018). Nevertheless, we apply the parameterization by Sitch et al. (2007) because the damage is reasonably associated with ambient $O_3$ level, and the scheme has been extensively evaluated against available observations (Yue et al., 2017; Yue and Unger, 2018). Fixed damage for low (even zero) $O_3$ included in some PFTs in the decoupled scheme may result in overestimation of $O_3$-vegetation feedback in the global model.

**Deleted:** the

To our knowledge, this is the first time that the effect of $O_3$ damage to IPE is included in a fully coupled global chemistry-carbon-climate model. Both the F and linear schemes can simulate reasonable reductions in IPE compared to global meta-analysis, although with large uncertainties. The reduced IPE, as precursors, have insignificant effects on surface $O_3$ concentrations in eastern China (Fig. 5 and Fig. 6), likely because of high anthropogenic emissions that undermine the feedback of IPE changes to surface $O_3$. However, the reduced IPE weakens SOA radiative forcing and increases surface temperature in the eastern U.S., where biogenic SOAs provide important contributions to total aerosols (Fine et al., 2008; Goldstein et al., 2009). These results suggest that IPE feedback to the surface $O_3$ is quite uncertain and dependent on ambient precursors (anthropogenic vs. biogenic) and oxidizing capacity ($NO_x$-saturated vs. $NO_x$-limited).

Variations in meteorological parameters may also influence $O_3$-vegetation feedback. Plant stomata tend to close under drought stress to prevent water loss. As a result, dry climate may weaken $O_3$-vegetation feedback through regulation of stomatal conductance (Lin et al., 2019). The effects of drought cannot be evaluated using ModelE2-YIBs, which simulates climatology with small interannual variability. In the future, a chemical transport model (CTM) coupled with a dynamic vegetation model (such as GC-YIBs developed by Lei et al. (2020)) will be used to examine drought impacts by using observation-based meteorological forcings.

Despite these uncertainties, our analyses highlight the importance of $O_3$–vegetation interactions in surface $O_3$ concentrations. The feedback should be considered in regional and global air quality models for more realistic simulations. Furthermore, the effect of positive feedback on surface $O_3$ may potentially aggravate $O_3$ pollution in the future with increased ambient $O_3$ under a warming climate (Lei et al., 2012; Doherty et al., 2013).

## Data availability

The observed hourly ozone concentrations for AQMN-MEE, CASTNET and EMEP were obtained from the Data Center of China's Ministry of Ecology and Environment (http://datacenter.mee.gov.cn/websjzx/queryIndex.vm), U.S. Environmental Protection Agency (https://java.epa.gov/castnet/clearsession.do) and EMEP Chemical Coordinating Centre (https://www.emep.int/). The source codes for the ModelE2-YIBs are available through collaboration. Please submit a request to X. Yue (yuexu@nuist.edu.cn).

## Author contribution

XY conceived the study. CG carried out the simulations and performed the analysis. YL and YM provided useful comments on the paper. CG, XY and HL prepared the manuscript with contributions from all coauthors.

## Competing interests

The authors declare that they have no conflict of interest.

## Acknowledgments

This work was supported by the National Key Research and Development Program of China (grant no. 2019YFA0606802) and the National Natural Science Foundation of China (grant nos. 41975155 and 91744311).

**Deleted:** , 91544219,

**Deleted:** , and 41475137) and National Key Research and Development Program of China (grant no. SQ2019YFA060013-02).

## References

Ainsworth, E. A., Yendrek, C. R., Sitch, S., Collins, W. J., and Emberson, L. D.: The Effects of Tropospheric Ozone on Net Primary Productivity and Implications for Climate Change, in: Annual Review of Plant Biology, Vol 63, edited by: Merchant, S. S., Annual Review of Plant Biology, 637-661, 2012.

Arneth, A., Niinemets, U., Pressley, S., Back, J., Hari, P., Karl, T., Noe, S., Prentice, I. C., Serca, D., Hickler, T., Wolf, A., and Smith, B.: Process-based estimates of terrestrial ecosystem isoprene emissions: incorporating the effects of a direct CO2-isoprene interaction, Atmospheric Chemistry and Physics, 7, 31-53, 10.5194/acp-7-31-2007, 2007.

Atkinson, R.: Atmospheric chemistry of VOCs and NOx, Atmospheric Environment, 34, 2063-2101, 10.1016/s1352-2310(99)00460-4, 2000.

Ball, J. T., Woodrow, I. E., and Berry, J. A.: A model predicting stomatal conductance and its contribution to the control of photosynthesis under different environmental conditions, Progress in Photosynthesis Research, 4, 221-224, 1987.

Bian, H. S., Prather, M. J., and Takemura, T.: Tropospheric aerosol impacts on trace gas budgets through photolysis, Journal of Geophysical Research-Atmospheres, 108, 10.1029/2002jd002743, 2003.

Broich, M., Huete, A., Paget, M., Ma, X., Tulbure, M., Coupe, N. R., Evans, B., Beringer, J., Devadas, R., Davies, K., and Held, A.: A spatially explicit land surface phenology data product for science, monitoring and natural resources management applications, Environmental Modelling & Software, 64, 191-204, 10.1016/j.envsoft.2014.11.017, 2015.

Calfapietra, C., Mugnozza, G. S., Karnosky, D. F., Loreto, F., and Sharkey, T. D.: Isoprene emission rates under elevated CO(2) and O(3) in two field-grown aspen clones differing in their sensitivity to O(3), New Phytologist, 179, 55-61, 10.1111/j.1469-8137.2008.02493.x, 2008.

Calfapietra, C., Fares, S., and Lofeto, F.: Volatile organic compounds from Italian vegetation and their interaction with ozone, Environmental Pollution, 157, 1478-1486, 10.1016/j.envpol.2008.09.048, 2009.

Calfapietra, C., Fares, S., Manes, F., Morani, A., Sgrigna, G., and Loreto, F.: Role of Biogenic Volatile Organic Compounds (BVOC) emitted by urban trees on ozone concentration in cities: A review, Environmental Pollution, 183, 71-80, 10.1016/j.envpol.2013.03.012, 2013.

Charlson, R. J., Schwartz, S. E., Hales, J. M., Cess, R. D., Coakley, J. A., Hansen, J. E., and Hofmann, D. J.: CLIMATE FORCING BY ANTHROPOGENIC AEROSOLS, Science, 255, 423-430, 10.1126/science.255.5043.423, 1992.

Chung, S. H., and Seinfeld, J. H.: Global distribution and climate forcing of carbonaceous aerosols, Journal of Geophysical Research-Atmospheres, 107, 10.1029/2001jd001397, 2002.

Claeys, M., Graham, B., Vas, G., Wang, W., Vermeylen, R., Pashynska, V., Cafmeyer, J., Guyon, P., Andreae, M. O., Artaxo, P., and Maenhaut, W.: Formation of secondary organic aerosols through photooxidation of isoprene, Science, 303, 1173-1176, 10.1126/science.1092805, 2004.

Collatz, G. J., Ball, J. T., Grivet, C., and Berry, J. A.: PHYSIOLOGICAL AND ENVIRONMENTAL-REGULATION OF STOMATAL CONDUCTANCE, PHOTOSYNTHESIS AND TRANSPIRATION - A MODEL THAT INCLUDES A LAMINAR BOUNDARY-LAYER, Agricultural and Forest Meteorology, 54, 107-136, 10.1016/0168-1923(91)90002-8, 1991.

Doherty, R. M., Wild, O., Shindell, D. T., Zeng, G., MacKenzie, I. A., Collins, W. J., Fiore, A. M., Stevenson, D. S., Dentener, F. J., Schultz, M. G., Hess, P., Derwent, R. G., and Keating, T. J.: Impacts of climate change on surface ozone and intercontinental ozone pollution: A multi-model study, Journal of Geophysical Research-Atmospheres, 118, 3744-3763, 10.1002/jgrd.50266, 2013.

Fares, S., Oksanen, E., Lannenpaa, M., Julkunen-Tiitto, R., and Loreto, F.: Volatile emissions and phenolic compound concentrations along a vertical profile of Populus nigra leaves exposed to realistic ozone concentrations, Photosynthesis Research, 104, 61-74, 10.1007/s11120-010-9549-5, 2010.

Farquhar, G. D., Caemmerer, S. V., and Berry, J. A.: A BIOCHEMICAL-MODEL OF PHOTOSYNTHETIC CO2 ASSIMILATION IN LEAVES OF C-3 SPECIES, Planta, 149, 78-90, 10.1007/bf00386231, 1980.

Feng, Z., Shang, B., Gao, F., and Calatayud, V.: Current ambient and elevated ozone effects on poplar: A global meta-analysis and response relationships, Science of the Total Environment, 654, 832-840, 10.1016/j.scitotenv.2018.11.179, 2019a.

Feng, Z., Yuan, X., Fares, S., Loreto, F., Li, P., Hoshika, Y., and Paoletti, E.: Isoprene is more affected by climate drivers than monoterpenes: A meta-analytic review on plant isoprenoid emissions, Plant Cell and Environment, 42, 1939-1949, 10.1111/pce.13535, 2019b.

Fine, P. M., Sioutas, C., and Solomon, P. A.: Secondary particulate matter in the United States: Insights from the particulate matter supersites program and related studies, Journal of the Air & Waste Management Association, 58, 234-253, 10.3155/1047-3289.58.2.234, 2008.

Fu, Y., and Liao, H.: Simulation of the interannual variations of biogenic emissions of volatile organic compounds in China: Impacts on tropospheric ozone and secondary organic aerosol, Atmospheric Environment, 59, 170-185, 10.1016/j.atmosenv.2012.05.053, 2012.

Fuhrer, J., Skarby, L., and Ashmore, M. R.: Critical levels for ozone effects on vegetation in Europe, Environmental Pollution, 97, 91-106, 10.1016/s0269-7491(97)00067-5, 1997.

Gauderman, W. J., Avol, E., Gilliland, F., Vora, H., Thomas, D., Berhane, K., McConnell, R., Kuenzli, N., Lurmann, F., Rappaport, E., Margolis, H., Bates, D., and Peters, J.: The effect of air pollution on lung development from 10 to 18 years of age, New England Journal of Medicine, 351, 1057-1067, 10.1056/NEJMoa040610, 2004.

Goldstein, A. H., Koven, C. D., Heald, C. L., and Fung, I. Y.: Biogenic carbon and anthropogenic pollutants combine to form a cooling haze over the southeastern United States, Proceedings of the National Academy of Sciences of the United States of America, 106, 8835-8840, 10.1073/pnas.0904128106, 2009.

Gregg, J. W., Jones, C. G., and Dawson, T. E.: Physiological and developmental effects of O-3 on cottonwood growth in urban and rural sites, Ecological Applications, 16, 2368-2381, 10.1890/1051-0761(2006)016[2368:padeoo]2.0.co;2, 2006.

Guenther, A., Karl, T., Harley, P., Wiedinmyer, C., Palmer, P. I., and Geron, C.: Estimates of global terrestrial isoprene emissions using MEGAN (Model of Emissions of Gases and Aerosols from Nature), Atmospheric Chemistry and Physics, 6, 3181-3210, 10.5194/acp-6-3181-2006, 2006.

Guenther, A. B., Jiang, X., Heald, C. L., Sakulyanontvittaya, T., Duhl, T., Emmons, L. K., and Wang, X.: The Model of Emissions of Gases and Aerosols from Nature version 2.1 (MEGAN2.1): an extended and updated framework for modeling biogenic emissions, Geoscientific Model Development, 5, 1471-1492, 10.5194/gmd-5-1471-2012, 2012.

Henze, D. K., and Seinfeld, J. H.: Global secondary organic aerosol from isoprene oxidation, Geophysical Research Letters, 33, 10.1029/2006gl025976, 2006.

Hartikainen, K., Nerg, A.-M., Kivimaenpaa, M., Kontunen-Soppela, S., Maenpaa, M., Oksanen, E., Rousi, M., and Holopainen, T.: Emissions of volatile organic compounds and leaf structural characteristics of European aspen (Populus tremula) grown under elevated ozone and temperature, Tree Physiology, 29, 1163-1173, 10.1093/treephys/tpp033, 2009.

Jacob, D. J., and Winner, D. A.: Effect of climate change on air quality, Atmospheric Environment, 43, 51-63, 10.1016/j.atmosenv.2008.09.051, 2009.

Koch, D., Schmidt, G. A., and Field, C. V.: Sulfur, sea salt, and radionuclide aerosols in GISS ModelE, Journal of Geophysical Research-Atmospheres, 111, 10.1029/2004jd005550, 2006.

Lamarque, J. F., Emmons, L. K., Hess, P. G., Kinnison, D. E., Tilmes, S., Vitt, F., Heald, C. L., Holland, E. A., Lauritzen, P. H., Neu, J., Orlando, J. J., Rasch, P. J., and Tyndall, G. K.: CAM-chem: description and evaluation of interactive atmospheric chemistry in the Community Earth System Model, Geoscientific Model Development, 5, 369-411, 10.5194/gmd-5-369-2012, 2012.

Lamarque, J. F., Shindell, D. T., Josse, B., Young, P. J., Cionni, I., Eyring, V., Bergmann, D., Cameron-Smith, P., Collins, W. J., Doherty, R., Dalsoren, S., Faluvegi, G., Folberth, G., Ghan, S. J., Horowitz, L. W., Lee, Y. H., MacKenzie, I. A., Nagashima, T., Naik, V., Plummer, D., Righi, M., Rumbold, S. T., Schulz, M., Skeie, R. B., Stevenson, D. S., Strode, S., Sudo, K., Szopa, S., Voulgarakis, A., and Zeng, G.: The Atmospheric Chemistry and Climate Model Intercomparison Project (ACCMIP): overview and description of models, simulations and climate diagnostics, Geoscientific Model Development, 6, 179-206, 10.5194/gmd-6-179-2013, 2013.

Lane, T. E., Donahue, N. M., and Pandis, S. N.: Effect of NOx on secondary organic aerosol concentrations, Environmental Science & Technology, 42, 6022-6027, 10.1021/es703225a, 2008.

Lei, H., Wuebbles, D. J., and Liang, X.-Z.: Projected risk of high ozone episodes in 2050, Atmospheric Environment, 59, 567-577, 10.1016/j.atmosenv.2012.05.051, 2012.

Lei, Y., Yue, X., Liao, H., Gong, C., and Zhang, L.: Implementation of Yale Interactive terrestrial Biosphere model v1.0 into GEOS-Chem v12.0.0: a tool for biosphere-chemistry interactions, Geosci. Model Dev., https://doi.org/10.5194/gmd-2019-281, in press, 2020.

Lelieveld, J., Evans, J. S., Fnais, M., Giannadaki, D., and Pozzer, A.: The contribution of outdoor air pollution sources to premature mortality on a global scale, Nature, 525, 367-371, 10.1038/nature15371, 2015.

Li, K., Jacob, D. J., Liao, H., Shen, L., Zhang, Q., and Bates, K. H.: Anthropogenic drivers of 2013-2017 trends in summer surface ozone in China, Proceedings of the National Academy of Sciences of the United States of America, 116, 422-427, 10.1073/pnas.1812168116, 2019.

Lin, M., Malyshev, S., Shevliakova, E., Paulot, F., Horowitz, L. W., Fares, S., Mikkelsen, T. N., and Zhang, L.: Sensitivity of Ozone Dry Deposition to Ecosystem-Atmosphere Interactions: A Critical Appraisal of Observations and Simulations, Global Biogeochemical Cycles, 33, 1264-1288, 10.1029/2018gb006157, 2019.

Liu, Z. Y., Notaro, M., Kutzbach, J., and Liu, N.: Assessing global vegetation-climate feedbacks from observations, Journal of Climate, 19, 787-814, 10.1175/jcli3658.1, 2006.

Lombardozzi, D., Levis, S., Bonan, G., and Sparks, J. P.: Predicting photosynthesis and transpiration responses to ozone: decoupling modeled photosynthesis and stomatal conductance, Biogeosciences, 9, 3113-3130, 10.5194/bg-9-3113-2012, 2012.

**Deleted:** -+,

Lombardozzi, D., Levis, S., Bonan, G., Hess, P. G., and Sparks, J. P.: The Influence of Chronic Ozone Exposure on Global Carbon and Water Cycles, Journal of Climate, 28, 292-305, 10.1175/jcli-d-14-00223.1, 2015.

Lu, X., Hong, J. Y., Zhang, L., Cooper, O. R., Schultz, M. G., Xu, X. B., Wang, T., Gao, M., Zhao, Y. H., and Zhang, Y. H.: Severe Surface Ozone Pollution in China: A Global Perspective, Environmental Science & Technology Letters, 5, 487-494, 10.1021/acs.estlett.8b00366, 2018.

Menon, S., Unger, N., Koch, D., Francis, J., Garrett, T., Sednev, I., Shindell, D., and Streets, D.: Aerosol climate effects and air quality impacts from 1980 to 2030, Environmental Research Letters, 3, 10.1088/1748-9326/3/2/024004, 2008.

Menon, S., Koch, D., Beig, G., Sahu, S., Fasullo, J., and Orlikowski, D.: Black carbon aerosols and the third polar ice cap, Atmospheric Chemistry and Physics, 10, 4559-4571, 10.5194/acp-10-4559-2010, 2010.

Moore, C. E., Brown, T., Keenan, T. F., Duursma, R. A., van Dijk, A. I. J. M., Beringer, J., Culvenor, D., Evans, B., Huete, A., Hutley, L. B., Maier, S., Restrepo-Coupe, N., Sonnentag, O., Specht, A., Taylor, J. R., van Gorsel, E., and Liddell, M. J.: Reviews and syntheses: Australian vegetation phenology: new insights from satellite remote sensing and digital repeat photography, Biogeosciences, 13, 5085-5102, 10.5194/bg-13-5085-2016, 2016.

Paoletti, E., and Grulke, N. E.: Does living in elevated CO2 ameliorate tree response to ozone? A review on stomatal responses, Environmental Pollution, 137, 483-493, 10.1016/j.envpol.2005.01.035, 2005.

Potter, C. S., Alexander, S. E., Coughlan, J. C., and Klooster, S. A.: Modeling biogenic emissions of isoprene: exploration of model drivers, climate control algorithms, and use of global satellite observations, Atmospheric Environment, 35, 6151-6165, 10.1016/s1352-2310(01)00390-9, 2001.

Presto, A. A., Hartz, K. E. H., and Donahue, N. M.: Secondary organic aerosol production from terpene ozonolysis. 2. Effect of NOx concentration, Environmental Science & Technology, 39, 7046-7054, 10.1021/es050400s, 2005.

Ryan, A., Cojocariu, C., Possell, M., Davies, W. J., and Hewitt, C. N.: Defining hybrid poplar (Populus deltoides x Populus trichocarpa) tolerance to ozone: identifying key parameters, Plant Cell and Environment, 32, 31-45, 10.1111/j.1365-3040.2008.01897.x, 2009.

Sadiq, M., Tai, A. P. K., Lombardozzi, D., and Martin, M. V.: Effects of ozone-vegetation coupling on surface ozone air quality via biogeochemical and meteorological feedbacks, Atmospheric Chemistry and Physics, 17, 3055-3066, 10.5194/acp-17-3055-2017, 2017.

Schmidt, G. A., Kelley, M., Nazarenko, L., Ruedy, R., Russell, G. L., Aleinov, I., Bauer, M., Bauer, S. E., Bhat, M. K., Bleck, R., Canuto, V., Chen, Y.-H., Cheng, Y., Clune, T. L., Del Genio, A., de Fainchtein, R., Faluvegi, G., Hansen, J. E., Healy, R. J., Kiang, N. Y., Koch, D., Lacis, A. A., LeGrande, A. N., Lerner, J., Lo, K. K., Matthews, E. E., Menon, S., Miller, R. L., Oinas, V., Oloso, A. O., Perlwitz, J. P., Puma, M. J., Putman, W. M., Rind, D., Romanou, A., Sato, M., Shindell, D. T., Sun, S., Syed, R. A., Tausnev, N., Tsigaridis, K., Unger, N., Voulgarakis, A., Yao, M.-S., and Zhang, J.: Configuration and assessment of the GISS ModelE2 contributions to the CMIP5 archive, Journal of Advances in Modeling Earth Systems, 6, 141-184, 10.1002/2013ms000265, 2014.

Sellers, P. J., Los, S. O., Tucker, C. J., Justice, C. O., Dazlich, D. A., Collatz, G. J., and Randall, D. A.: A revised land surface parameterization (SiB2) for atmospheric GCMs .2. The generation of global fields of terrestrial biophysical parameters from satellite data, Journal of Climate, 9, 706-737, 10.1175/1520-0442(1996)009<0706:arlspf>2.0.co;2, 1996.

Sillman, S.: The relation between ozone, NOx and hydrocarbons in urban and polluted rural environments, Atmospheric Environment, 33, 1821-1845, 10.1016/s1352-2310(98)00345-8, 1999.

Sitch, S., Cox, P. M., Collins, W. J., and Huntingford, C.: Indirect radiative forcing of climate change through ozone effects on the land-carbon sink, Nature, 448, 791-U794, 10.1038/nature06059, 2007.

Spitters, C. J. T., Toussaint, H., and Goudriaan, J.: SEPARATING THE DIFFUSE AND DIRECT COMPONENT OF GLOBAL RADIATION AND ITS IMPLICATIONS FOR MODELING CANOPY PHOTOSYNTHESIS .1. COMPONENTS OF INCOMING RADIATION, Agricultural and Forest Meteorology, 38, 217-229, 10.1016/0168-1923(86)90060-2, 1986.

Sun, Y., Zhuang, G., Tang, A., Wang, Y., and An, Z.: Chemical characteristics of PM2.5 and PM10 in haze-fog episodes in Beijing, Environmental Science & Technology, 40, 3148-3155, 10.1021/es051533g, 2006.

Tiiva, P., Rinnan, R., Holopainen, T., Morsky, S. K., and Holopainen, J. K.: Isoprene emissions from boreal peatland microcosms; effects of elevated ozone concentration in an open field experiment, Atmospheric Environment, 41, 3819-3828, 10.1016/j.atmosenv.2007.01.005, 2007.

Tucker, C. J., Slayback, D. A., Pinzon, J. E., Los, S. O., Myneni, R. B., and Taylor, M. G.: Higher northern latitude normalized difference vegetation index and growing season trends from 1982 to 1999, International Journal of Biometeorology, 45, 184-190, 10.1007/s00484-001-0109-8, 2001.

Unger, N.: Isoprene emission variability through the twentieth century, Journal of Geophysical Research-Atmospheres, 118, 13606-13613, 10.1002/2013jd020978, 2013.

Unger, N., Harper, K., Zheng, Y., Kiang, N. Y., Aleinov, I., Arneth, A., Schurgers, G., Amelynck, C., Goldstein, A., Guenther, A., Heinesch, B., Hewitt, C. N., Karl, T., Laffineur, Q., Langford, B., McKinney, K. A., Misztal, P., Potosnak, M., Rinne, J., Pressley, S., Schoon, N., and Seraca, D.: Photosynthesis-dependent isoprene emission from leaf to planet in a global carbon-chemistry-climate model, Atmospheric Chemistry and Physics, 13, 10243-10269, 10.5194/acp-13-10243-2013, 2013

Moved (insertion) [2]

Val Martin, M., Heald, C. L., and Arnold, S. R.: Coupling dry deposition to vegetation phenology in the Community Earth SystemModel: Implications for the simulation of surface O3, Geophysical Research Letters, 41, 2988-2996, 10.1002/2014gl059651, 2014.

van Vuuren, D. P., Edmonds, J., Kainuma, M., Riahi, K., Thomson, A., Hibbard, K., Hurtt, G. C., Kram, T., Krey, V., Lamarque, J.-F., Masui, T., Meinshausen, M., Nakicenovic, N., Smith, S. J., and Rose, S. K.: The representative concentration pathways: an overview, Climatic Change, 109, 5-31, 10.1007/s10584-011-0148-z, 2011.

Velikova, V., Tsonev, T., Pinelli, P., Alessio, G. A., and Loreto, F.: Localized ozone fumigation system for studying ozone effects on photosynthesis, respiration, electron transport rate and isoprene emission in field-grown Mediterranean oak species, Tree Physiology, 25, 1523-1532, 10.1093/treephys/25.12.1523, 2005.

Wang, G., Huang, Y., Wei, Y., Zhang, W., Li, T., and Zhang, Q.: Climate Warming Does Not Always Extend the Plant Growing Season in Inner Mongolian Grasslands: Evidence From a 30-Year In Situ Observations at Eight Experimental Sites, Journal of Geophysical Research-Biogeosciences, 124, 2364-2378, 10.1029/2019jg005137, 2019.

Wang, T., Xue, L., Brimblecombe, P., Lam, Y. F., Li, L., and Zhang, L.: Ozone pollution in China: A review of concentrations, meteorological influences, chemical precursors, and effects, Sci Total Environ, 575, 1582-1596, 10.1016/j.scitotenv.2016.10.081, 2017.

Wesely, M. L.: PARAMETERIZATION OF SURFACE RESISTANCES TO GASEOUS DRY DEPOSITION IN REGIONAL-SCALE NUMERICAL-MODELS, Atmospheric Environment, 23, 1293-1304, 10.1016/0004-6981(89)90153-4, 1989.

Wesely, M. L., and Hicks, B. B.: A review of the current status of knowledge on dry deposition, Atmospheric Environment, 34, 2261-2282, 10.1016/s1352-2310(99)00467-7, 2000.

White, M. A., Nemani, R. R., Thornton, P. E., and Running, S. W.: Satellite evidence of phenological differences between urbanized and rural areas of the eastern United States deciduous broadleaf forest, Ecosystems, 5, 260-273, 10.1007/s10021-001-0070-8, 2002.

Wittig, V. E., Ainsworth, E. A., and Long, S. P.: To what extent do current and projected increases in surface ozone affect photosynthesis and stomatal conductance of trees? A meta-analytic review of the last 3 decades of experiments, Plant Cell and Environment, 30, 1150-1162, 10.1111/j.1365-3040.2007.01717.x, 2007.

Wu, L., Zhang, J., and Dong, W.: Vegetation effects on mean daily maximum and minimum surface air temperatures over China, Chinese Science Bulletin, 56, 900-905, 10.1007/s11434-011-4349-7, 2011.

Xiao, X., Hagen, S., Zhang, Q., Keller, M., and Moore, B., III: Detecting leaf phenology of seasonally moist tropical forests in South America with multi-temporal MODIS images, Remote Sensing of Environment, 103, 465-473, 10.1016/j.rse.2006.04.013, 2006.

Yang, F., Tan, J., Zhao, Q., Du, Z., He, K., Ma, Y., Duan, F., Chen, G., and Zhao, Q.: Characteristics of PM2.5 speciation in representative megacities and across China, Atmospheric Chemistry and Physics, 11, 5207-5219, 10.5194/acp-11-5207-2011, 2011.

Yin, C., Pu, X., Xiao, Q., Zhao, C., and Liu, Q.: Effects of night warming on spruce root around non-growing season vary with branch order and month, Plant and Soil, 380, 249-263, 10.1007/s11104-014-2090-0, 2014.

Yuan, X., Calatayud, V., Gao, F., Fares, S., Paoletti, E., Tian, Y., and Feng, Z.: Interaction of drought and ozone exposure on isoprene emission from extensively cultivated poplar, Plant Cell and Environment, 39, 2276-2287, 10.1111/pce.12798, 2016.

Yuan, X., Feng, Z., Liu, S., Shang, B., Li, P., Xu, Y., and Paoletti, E.: Concentration-and flux-based dose-responses of isoprene emission from poplar leaves and plants exposed to an ozone concentration gradient, Plant Cell and Environment, 40, 1960-1971, 10.1111/pce.13007, 2017.

Yue, X., and Unger, N.: Ozone vegetation damage effects on gross primary productivity in the United States, Atmospheric Chemistry and Physics, 14, 9137-9153, 10.5194/acp-14-9137-2014, 2014.

Yue, X., and Unger, N.: The Yale Interactive terrestrial Biosphere model version 1.0: description, evaluation and implementation into NASA GISS ModelE2, Geoscientific Model Development, 8, 2399-2417, 10.5194/gmd-8-2399-2015, 2015.

Yue, X., Keenan, T. F., Munger, W., and Unger, N.: Limited effect of ozone reductions on the 20-year photosynthesis trend at Harvard forest, Global Change Biology, 22, 3750-3759, 10.1111/gcb.13300, 2016.

Yue, X., Unger, N., Harper, K., Xia, X., Liao, H., Zhu, T., Xiao, J., Feng, Z., and Li, J.: Ozone and haze pollution weakens net primary productivity in China, Atmospheric Chemistry and Physics, 17, 6073-6089, 10.5194/acp-17-6073-2017, 2017.

Yue, X., and Unger, N.: Fire air pollution reduces global terrestrial productivity, Nature Communications, 9, 5413, 10.1038/s41467-018-07921-4, 2018.

Zhou, S. S., Tai, A. P. K., Sun, S., Sadiq, M., Heald, C. L., and Geddes, J. A.: Coupling between surface ozone and leaf area index in a chemical transport model: strength of feedback and implications for ozone air quality and vegetation health, Atmospheric Chemistry and Physics, 18, 14133-14148, 10.5194/acp-18-14133-2018, 2018.

**Deleted:** Unger, N., Harper, K., Xia, X., Liao, H., Zhu, T., Xiao, J., Feng, Z., and Li, J.: Ozone and haze pollution weakens net primary productivity in China, Atmospheric Chemistry and Physics, 17, 6073-6089, 10.5194/acp-17-6073-2017, 2017

**Deleted:** Zheng, B., Tong, D., Li, M., Liu, F., Hong, C., Geng, G., Li, H., Li…

**Deleted:** Yan, L., Zhang, Y., Zhao, H

**Moved up [2]:** ., Zheng, Y.,

**Deleted:** Peng, L., Qi

**Deleted:** He, K.,

**Deleted:** Zhang, Q.: Trends

**Deleted:** China's anthropogenic emissions since 2010 as the consequence of clean air actions

**Deleted:** 18, 14095-14111

**Deleted:** 18-14095-2018

## Tables

**Table 1. Summary of the seven experiments in ModelE2-YIBs.**

| Name | $O_3$ damage to photosynthesis | $O_3$ damage to stomatal conductance | $O_3$ damage to isoprene emissions |
|---|---|---|---|
| CTRL | Offline | Offline | Linear (offline) |
| DRY_high | F_high | F_high | F_high (offline) |
| DRY_ low | F_low | F_low | F_low (offline) |
| TOTAL_F_high | F_high | F_high | F_high |
| TOTAL_F_low | F_low | F_low | F_low |
| TOTAL_LINEAR_high | F_high | F_high | Linear |
| TOTAL_LINEAR_low | F_low | F_low | Linear |

**Deleted:** None

**Deleted:** None

**Figures**

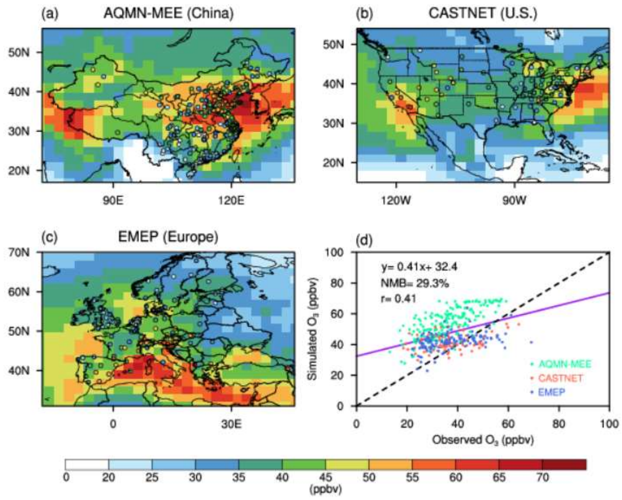

**Figure 1. Evaluations of simulated summer surface $O_3$ concentrations in the CTRL run. (a) - (c) Spatial distribution of observed $O_3$ concentrations (circle dots) in AQMN-MEE in China, CASTNET in the U.S. and EMEP in Europe, respectively, and the simulated $O_3$ concentrations. (d) Scatter plots of $O_3$ concentrations (ppbv) over observational sites in the three regions. The X and Y axes indicate the observed and simulated $O_3$ concentrations, respectively. The purple line shows the linear regression between the observed and simulated $O_3$ concentrations. The black dashed line shows the 1:1 lines.**

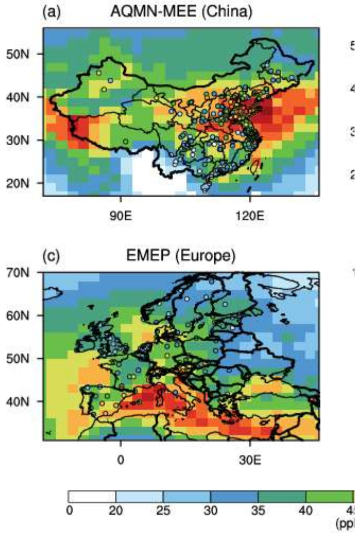

**Deleted:**

**Deleted:** red

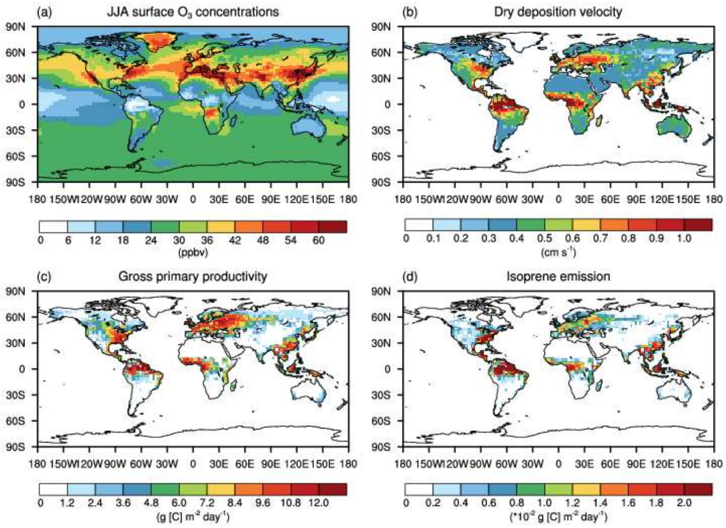

**Figure 2. The JJA-mean (a) surface O$_3$ concentrations, (b) O$_3$ dry deposition velocity, (c) gross primary productivity and (d) isoprene emissions in the CTRL simulation without O$_3$ damage to vegetation.**

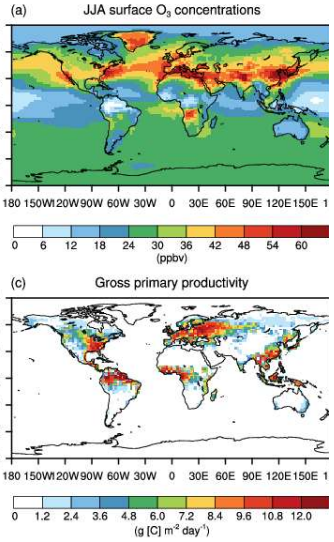

**Deleted:**

**Formatted:** Font color: Auto

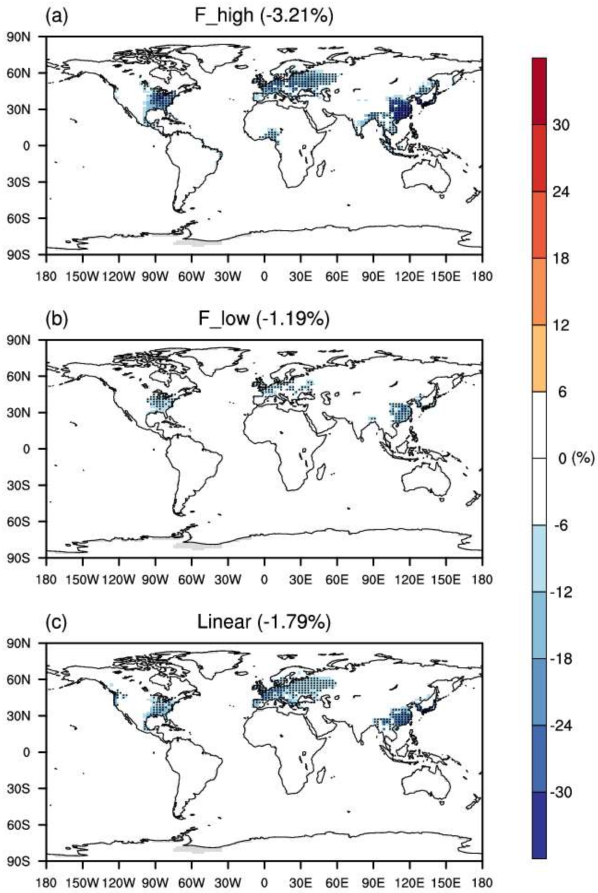

**Figure 3. Offline $O_3$ damage (%) to IPE averaged over summer using the F scheme with (a) high or (b) low sensitivities and results obtained by using the (c) linear scheme. The dotted grids shows significant damage at the 95% confidence level. Global land area-weighted percentage changes in IPE are shown in the titles.**

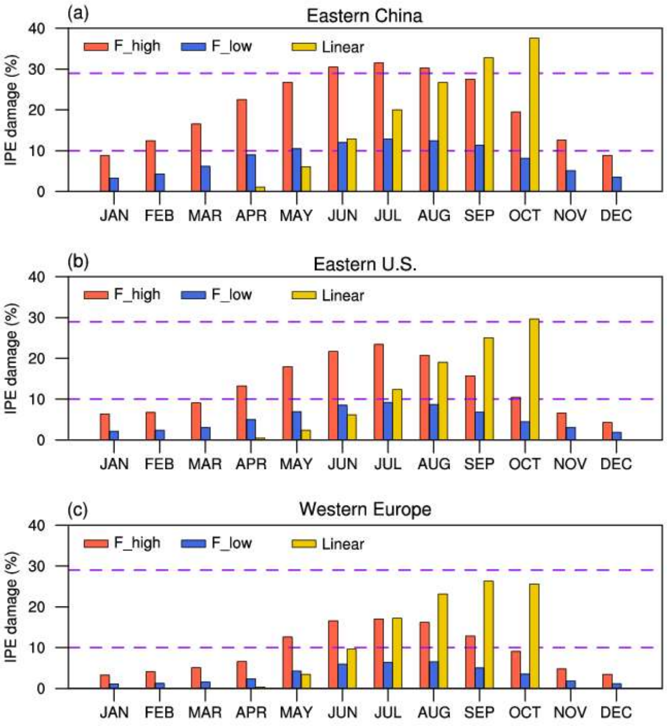

**Figure 4. Monthly mean percentage $O_3$ damage to IPE averaged over (a) eastern China, (b) the eastern U.S. and (c) western Europe by using the F scheme with high/low sensitivities and the linear scheme, respectively. The dashed lines indicate the range of IPE damage summarized by observational meta-analysis.**

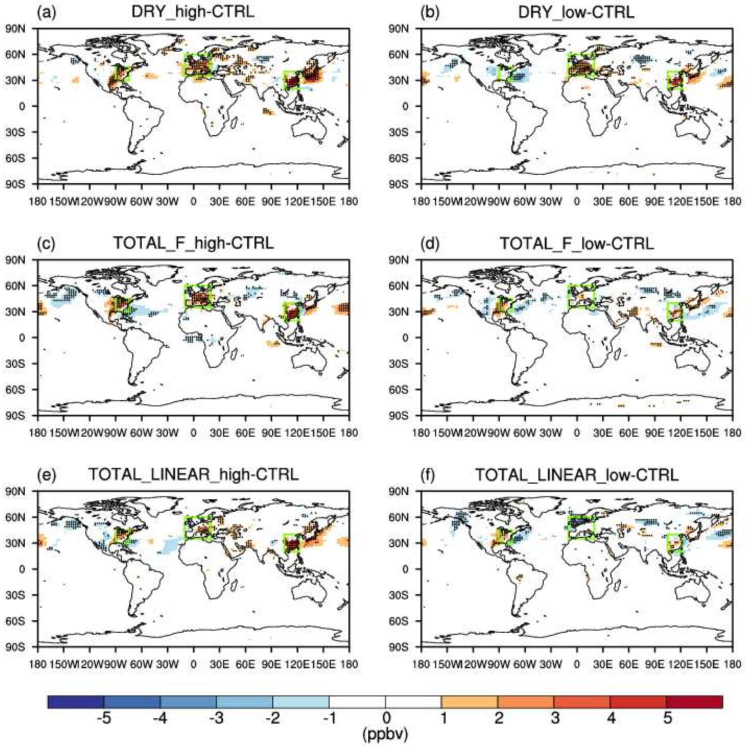

**Figure 5. O$_3$-vegetation feedback on surface O$_3$ concentrations during summer. The results shown are changes in surface O$_3$ resulting from O$_3$ damage to stomatal conductance alone with (a) high and (b) low sensitivity. In addition to stomatal conductance, O$_3$ damage to IPE is also included by using the F scheme with (c) high and (d) low sensitivity. In comparison, O$_3$ damage to IPE is added for the linear scheme in (e) and (f). The dotted grids indicate significant changes at the 95% confidence level. The three box regions denote eastern China, the eastern U.S., and western Europe.**

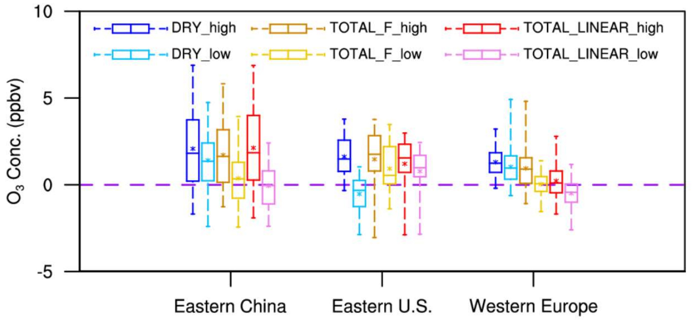

**Figure 6. Box plots of summer $O_3$ changes in three sensitive regions among different sensitivity experiments. The error bars show the ranges of $O_3$ changes in individual grids over the selected regions. Asterisks indicate the mean $O_3$ changes averaged over the selected regions.**

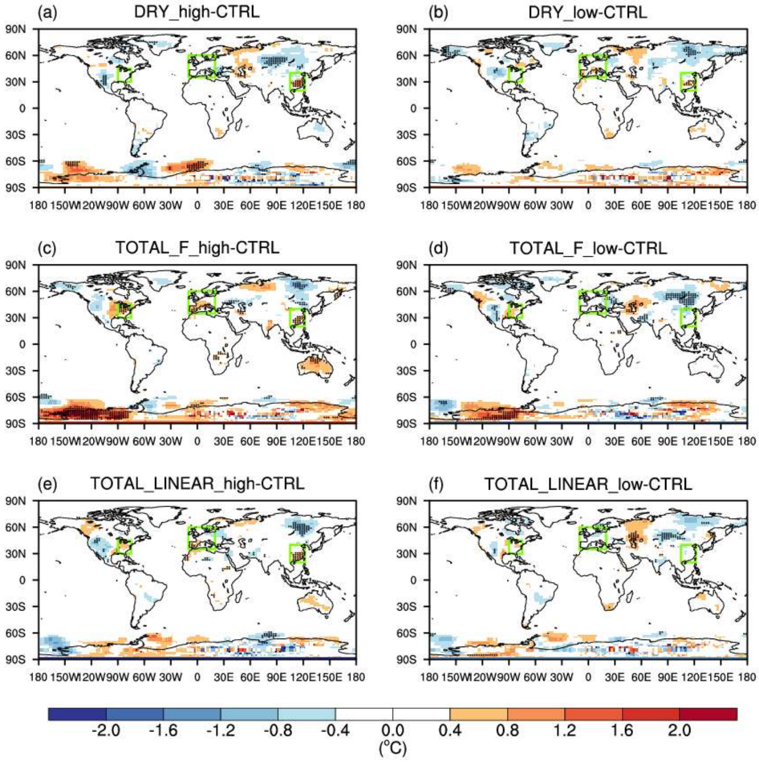

**Figure 7. Same as Fig. 5 but for changes in surface air temperature.**

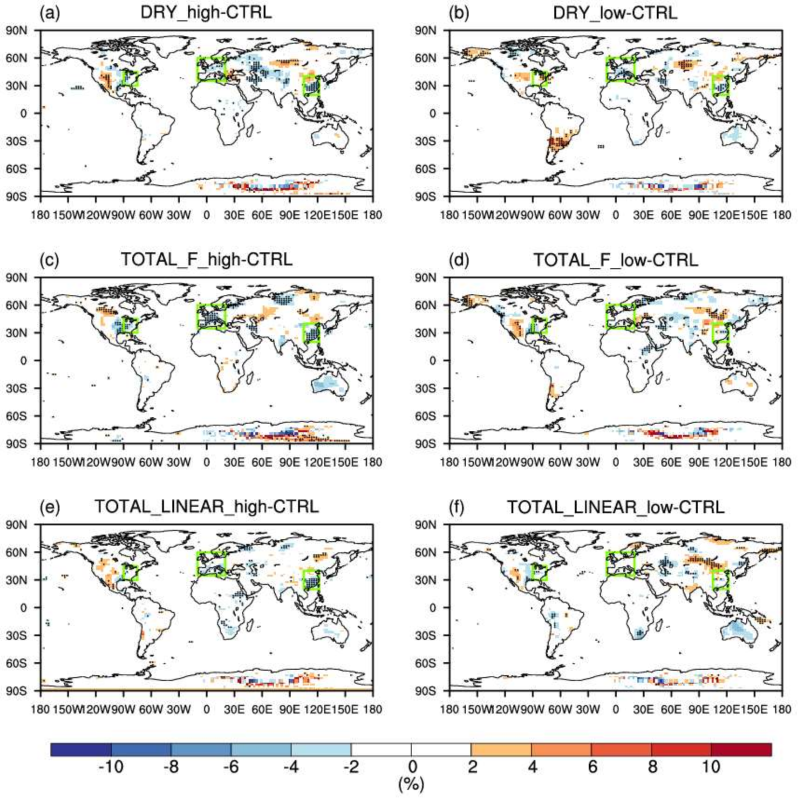

**Figure 8. Same as Fig. 5 but for changes in relatively humidity.**

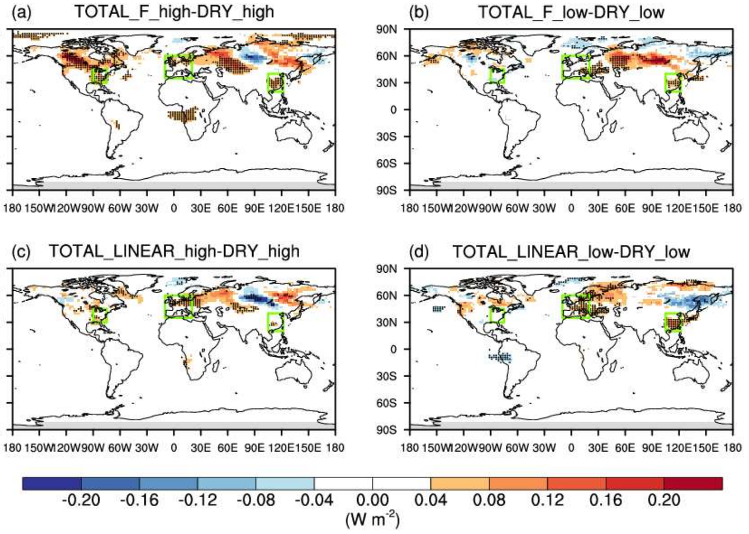

**Figure 9. Effects of $O_3$-induced IPE reductions on SOA shortwave radiative forcing at the surface during the boreal summer. The impacts of $O_3$ damage to IPE are isolated by determining the differences in the experiments for (a) high and (b) low sensitivities by using the F schemes or the (c, d) linear scheme. Dotted grids indicate significant changes at the 95% confidence level.**